Stanford University

Final Report
NASA NIAC Phase I Study

ReachBot: a Small Robot for Large Mobile Manipulation Tasks in Martian Cave Environments

Prepared for
NASA Innovative Advanced Concepts Program Office

Submitted January 11, 2022

Submitted by:
Prof. Marco Pavone, PI
Dep. of Aeronautics and Astronautics
Stanford University
Email: **pavone@stanford.edu**

Prof. Mark Cutkosky, Co-I
Dep. of Mechanical Engineering
Stanford University
cutkosky@stanford.edu

Prof. Mathieu Lapôtre, Co-I
Dep. of Geological Sciences
Stanford University
mlapotre@stanford.edu

Stephanie Schneider
Dep. of Aeronautics and Astronautics
Stanford University
schneids@stanford.edu

Tony G. Chen
Dep. of Mechanical Engineering
Stanford University
agchen@stanford.edu

Andrew Bylard
Dep. of Aeronautics and Astronautics
Stanford University
bylard@stanford.edu

Executive Summary

This study investigated a novel mission architecture where a long-reach crawling and anchoring robot, which repurposes extendable booms for mobile manipulation, is deployed to explore and sample difficult terrains on solar system bodies, with a key focus on Mars exploration. To this end, the robot concept introduced by this effort, called ReachBot, uses rollable extendable booms as manipulator arms and as highly reconfigurable structural members. ReachBot is capable of (1) rapid and versatile crawling through sequences of long-distance grasps, (2) traversing a large workspace while anchored (by adjusting boom lengths and orientations), and (3) applying high interaction forces and torques, primarily leveraging boom tensile strength and the variety of anchors within reach. These features allow a light and compact robot to achieve versatile mobility and forceful interaction in traditionally difficult environments such as vertical cliff walls or the rocky and uneven interiors of caves on Mars (see figure, left). In particular, ReachBot is uniquely suited for exploring and sampling Noachian targets on Mars that contain key sources of historical and astrobiological information preserved in strata in the form of cliff-face fractures and sublimation pits [1]. To develop this concept, this Phase I study brought together an interdisciplinary team of experts in robot autonomy, robotic manipulation, mechanical design, bio-inspired grasping, and geological planetary science from Stanford.

The Phase I study was aimed at providing an initial feasibility assessment of the proposed architecture and was structured around four key objectives necessary to demonstrate feasibility: (1) expand the reachable and wrench workspace through mechanical design trade-offs, (2) develop a robust control and motion planning strategy, (3) develop reliable surface grasping solutions, and (4) design a feasible mission architecture for exploration and sampling of Martian caves, with a particular focus on Noachian-era targets.

The main results of our study can be summarized as follows:

- **Expanded reachable workspace:** To showcase ReachBot's unique ability to access challenging terrain, we deployed it in a simulated environment with sparse anchor points that would be impassible for existing robots [2]. In the simulation, ReachBot followed a series of waypoints under nominal conditions, as well under conditions that exacerbate the common pitfalls of its feedback linearization controller. After injecting modeling errors and process disturbances,

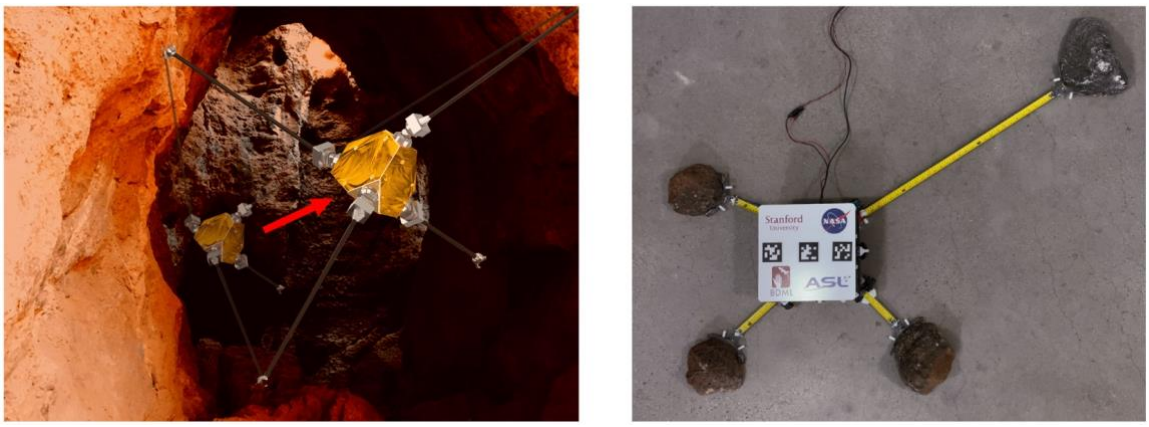

(Left) Concept image of ReachBot using its extendable boom arms to navigate the treacherous geometry of a Martian cavern. (Right) Planar ReachBot prototype using extendable measuring tape arms and microspine grippers to anchor the robot and to reach out and retrieve a rock sample.

ReachBot quickly converged back to the nominal trajectory. By empirically demonstrating good performance under adverse conditions, we verified (1) our controller provides acceptable performance, and (2) ReachBot can use its expanded reachable space to traverse terrain impassible for other robots, e.g. for robots with traditional rigid-link articulated arms.

- **Developed a robust controller and motion planning strategy:** By using extendable booms for mobility and manipulation, ReachBot provides a large reachable workspace with a lightweight and compact design. However, thin structural members like extended booms often have material properties that make them susceptible to buckling or bending failure. We overcome typical limitations by exploiting the booms' tensile strength. In this study, we demonstrated that applying uniform pretension to the booms increased system robustness. We then modified existing work in multi-fingered dexterous manipulation to explicitly control internal force and thus control pretension in the booms [2]. Drawing inspiration from successful climbing paradigms, we designed a controller that alternated between body movement and end-effector movement modes. The model for body movement was based on three constraining relationships: dynamics constraints, zero relative motion at contact, and static equilibrium at contact. We modified a feedback linearization controller for dexterous hands to design the body movement controller. For the end-effector movement stage, we modeled the end-effector as a point mass on a massless rod, and controlled it using a standard PD controller.
- **Developed reliable surface grasping solutions:** We performed experiments with rock grasping and coordinated locomotion on a 2D planar prototype to illustrate the advantages of low-inertia passive grippers, triggered by impact and using stored mechanical energy for the required internal grasping force (see figure, right). Gripper design involves a trade-off among the range of possible grasp angles, maximum grasp force, triggering force, and required reset force. Relocating the reset motor to the robot body permitted a low inertia (40g) prototype with a 25:1 ratio of maximum pull force to triggering force, limited only by the strength of the 3D printed components [3]. The same principles can be adapted to fully three-dimensional grasping with stronger materials in future work.
- **Designed a nominal mission architecture:** In the Phase I study, we performed a preliminary case study analysis for mission operations to Huo Hsing Vallis. At a high-level, the plan for mission operations includes two main phases. In the first phase, a lander or rover on the surface anchors at the edge of the cliff and lowers ReachBot on a tether. Then, ReachBot traverses the cavern floor, walls, and ceiling while inspecting stratified layers. The second phase includes three recurring tasks: (1) collect local scientific data, (2) take boom-tip pictures of environment to gather context information, and (3) extract and cache samples for return.

Through these investigations, we demonstrated that the bounding assumptions behind our proposed robot architecture are reasonable, with a sound scientific and engineering basis. A future study should focus on the key feasibility and maturation aspects identified during Phase I, in particular (1) optimizing the reachable workspace, (2) developing grasp site identification techniques and a 3D gripper prototype, (3) designing control strategies to mitigate risk, and (4) developing test procedures and testing the prototype in a realistic mission environment.

This study led to two publications:

- S. Schneider, A. Bylard, T. G. Chen, P. Wang, M. R. Cutkosky, M. Lapôtre, and M. Pavone. ReachBot: A small robot for large mobile manipulation tasks. In IEEE Aerospace Conference, 2022.
- T. G. Chen, B. Miller, C. Winston, S. Schneider, A. Bylard, M. Pavone, and M. R. Cutkosky. ReachBot: A small robot with exceptional reach for rough terrain. In Proc. IEEE Conf. on Robotics and Automation, 2022. Submitted.

Technical papers, related presentations, movies of the experiments, etc. can be found at the project's website: http://bdml.stanford.edu/Main/ReachBot.

Contents

1 Introduction

In this section, we motivate ReachBot and discuss its high-level design. Specifically, in Section 1.1, we motivate the need for a robot capable of versatile mobility and forceful manipulation in challenging environments and point out the technological gap in existing solutions. Then, in Section 1.2, we introduce the ReachBot concept at a high level and explain how ReachBot fills that gap.

1.1 Motivation

The recent decadal survey report for planetary science prioritizes three main crosscutting themes for planetary exploration: (1) the characterization of early solar system history, (2) the search for planetary habitats, and (3) an improved understanding about the nature of planetary processes [4]. Subsurface Martian caves and rocky outcrops have been identified as exploration targets to collectively address these three themes. Caves and cliffs offer protected environments with insulating and shielding properties that preserve ancient material in stratified layers. The stable conditions fostered by protected environments on Mars may also promote mineral precipitation and microbial growth. Therefore, these environments could provide key sources of historical and astrobiological information. Additionally, sheltered caves could provide sites for future human habitation of Mars. To characterize these environments, some measurements can be obtained with remote platforms (such as space telescopes or orbiting spacecraft), but many other essential measurements require direct contact with or close proximity to the surface. Furthermore, to maximize scientific gain, proximal measurements require precise targeting and access to remote or tight spaces. Hence, in-situ exploration is an important need in the scientific community. Specifically, to reveal geological history and search for signs of microbial life, the science goals of an in-situ mission to Martian caves or cliffs include wall stratigraphy and sample acquisition from different layers of bedrock.

To achieve these scientific goals, the objectives for a comprehensive in-situ study of Martian caves are threefold. First, a robot must traverse rough terrain on the floor, walls, and ceiling. Second, a robot must investigate relevant scientific targets, including reaching instruments into tight crevasses, performing contact measurements, and drilling into rock to collect samples. Third, a robot must record context of any measurements via remote sensing, e.g. by using a camera far from the target site to take an image the full scene.

Fulfilling these mission objectives requires a robot capable of precise, versatile mobility around challenging surface geometries as well as forceful and targeted manipulation. Current robotic platforms for cave exploration tend to be limited in mobility or manipulation capabilities, often sacrificing either accessibility or forceful manipulation. Platforms that rely on rolling [5, 6, 7] for mobility have limited accessibility of cave ceilings and overhanging walls, deferring to remote sensing for scientific investigation of such surfaces. For example, the Axel robot's wheeled rappelling design makes it unable to access overhanging surfaces or move reliably along a rocky floor [8]. Thus, it would not be able to perform complete wall stratigraphy or collect continuous samples from cliffs and caves. While hovering robots with perching capabilities [9, 10] are able to approach more varied terrain, they still have limited accessibility. In particular, without the ability to perch on ceilings and overhanging surfaces, they do not have the means to take contact measurements or apply forceful manipulation to targets on those surfaces. Separately, climbing robots use anchoring to traverse surfaces in opposition of gravity, enabling direct access to overhanging surface geometries as well as a brace for forceful manipulation. However, existing designs such as LEMUR [11] have short, bulky limbs that limit their reachable workspace. This limitation is incompatible with underground caves and cliffs on Mars where science targets may be located deep inside tight spaces or across expansive gaps. The need for a robot capable of navigating these environments motivates the development of a new robot design.

1.2 High-Level Concept

To navigate the difficult terrain of Martian caves and cliffs, our proposed solution, called ReachBot, uses extendable booms as manipulator arms and as highly reconfigurable structural members, as shown in Figure 1.1. It does this by merging two technologies that have had little previous overlap: mobile manipulation robots (e.g., LEMUR [11], RoboSimian [12], and Robonaut [13]) and lightweight extendable booms [14, 15], which have been primarily used for deployable space structures [16, 17]. This combination addresses a key technology gap in robots for space missions, where compact and lightweight designs are prized: small robots are often limited to both a small feasible workspace and small manipulator wrench (combination of force and torque) capability. Conversely, large robots can be more capable in these areas but are hampered by high mass and complexity. The ReachBot concept allows a small and lightweight robot to meet or exceed the reach and interaction force capabilities of a large robot. Adapting spine-based grasping from previous work [18, 11, 19], ReachBot attains mobility and forceful interaction in difficult but geologically interesting environments, such as overhanging or vertical surfaces in caves, cliffs, and other rock formations.

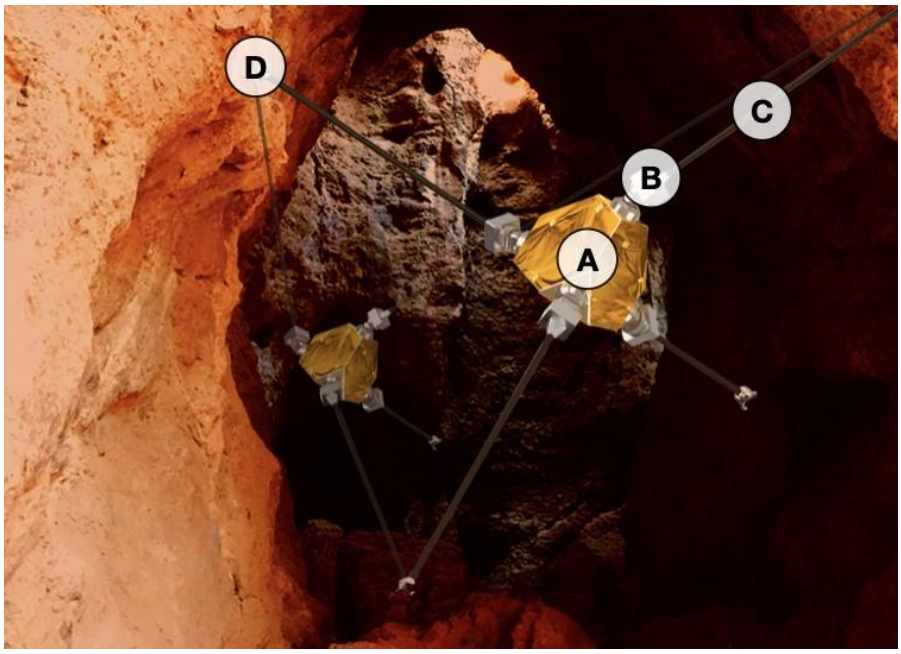

Figure 1.1: The ReachBot concept consists of a compact body (A) with long, extendable booms (B) on shoulder joints (C). The ends of the booms are equipped with small grippers (D) for attaching to rocky surfaces. After grasping, the booms can sustain large tensile loads.

ReachBot works by sequentially extending booms toward remote objects or surfaces, attaching a small end-effector, applying tension, and then releasing and repositioning one of the booms when ready for the next step. As in dexterous manipulation theory, ReachBot itself should remain under force closure [20, 21, 22]. With appropriate anchoring, the tensile forces can be large, enabling ReachBot to interact forcefully with its environment without risking instability.

ReachBot enables a mission with the afforementioned objectives by using microspine grippers to climb on floors, ceilings, and walls at any angle. ReachBot's small frame enables mobility in tight

spaces, while its large reach enables access to many more anchor points and scientific targets, demonstrating notable accessibility. ReachBot can also use extended booms as a lever arms to apply forceful manipulation, for example to brace itself while drilling into bedrock. Additionally, ReachBot can extend boom-mounted science instruments far from the robot body. These remote-sensing capabilities will enable overall mapping of the cave walls at multiple wavelengths as well as identification of targets for closer investigation. Proximal instruments mounted on the ends of booms also provide precision inspection into tight spaces where interesting astrobiological material is most likely to reside.

1.3 Structure of the Report

This report discusses our preliminary study of the ReachBot concept, and is structured as follows. In Section 2, we summarize our study of science objectives for potential ReachBot missions. In Section 3, we present our study of the ReachBot concept. We discuss the benefits and challenges of the design, and demonstrate its feasibility through modeling, simulation, and experiments on a hardware prototype. For each focus area, we identify future research directions for following studies. Then, in Section 4 we discuss the mission architecture and reference payloads in the context of a case study to explore Huo Hsing Vallis on Mars. Finally, in Section 5, we draw our conclusions and discuss key feasibility aspects to be considered in a future study.

2 ReachBot Science Objectives

In this section, we discuss the science objectives that motivate the development of ReachBot. In Section 2.1, we consider ReachBot's benefit in the context of the Martian subsurface and in Section 2.2, we consider its benefit in other environments.

2.1 Science Objectives in the Context of Mars Exploration

Mars is the most readily available Earth-like planet. It is thought that Mars was a lot more like the Earth $\sim$ 3.8 Gyr ago, with a thicker atmosphere and perhaps even a surface ocean. With its rich history and well-preserved record of geological and atmospheric processes, Mars is a prime exploration target that could help us understand the workings of a terrestrial planet without plate tectonics, and in doing so, teach us about the early Earth [23]. Because Earth's early geologic record has been destroyed by plate tectonics, Mars exploration is key to uncover a record of early planetary evolution that does not exist on Earth anymore. Unlike on Earth, a significant fraction of Mars's surface dates back to the period of time when life likely first evolved, providing an unparalleled window into the geological history of planetary evolution and habitability [24]. Additionally, early conditions on Mars are thought to have been conducive to the formation of prebiotic compounds, making Mars a valuable site to study the evolution of life and how it relates to the evolution of planets. The subsurface of Mars in particular is noted for being a promising target for biosignatures, both in terms of habitability and the preservation of biosignatures. To reconstruct Mars's geological and biological history, it is crucial not only to collect measurements and analyze samples, but also to have context of such data in a stratigraphic framework.

In the context of the 2013 Decadal survey *Vision and Voyages* on planetary science (compiled by the National Research Council [4]), ReachBot targets two themes that identify Mars as a key location of study.

- **The "Planetary Habitats" theme**, which aims to search for habitable environments that could host and sustain life, includes the questions: (1) What were the primordial sources of organic matter, and where does organic synthesis continue today? and (2) Beyond Earth, are there contemporary habitats elsewhere in the solar system with necessary conditions, organic matter, water, energy, and nutrients to sustain life, and do organisms live there now?

  ReachBot addresses these questions by focusing on Mars's subsurface, a promising target for habitability investigations. Even though it is thought that Mars's surface was habitable, there are unsolved and debated questions about temperature and timescales of the stability of liquid water. It could even be that the surface was never hospitable. The subsurface, however, provides heat, water, and geochemical gradients – everything that is needed for life to emerge. In addition, any biosignatures in the subsurface would have been shielded from billions of years of cosmic radiation. Thus, caves not only constitute a potential refugium for early life, but also an environment where the signatures of life could have been preserved over geologic timescales. By performing complete wall stratigraphy of cliffs and caverns, ReachBot targets the geological record of Mars's subsurface, which is crucial for studying how planetary evolution may relate to prebiotic and biotic processes.

- **The "Workings of Solar Systems" theme**, which aims to understand how geological, atmospheric, and possibly biological processes influence planetary evolution, includes the question:

  Can understanding the roles of physics, chemistry, geology, and dynamics in driving planetary atmospheres and climates lead to a better understanding of climate change on Earth?

Early conditions on Mars were likely similar to early conditions on Earth, and Mars still has the most Earth-like atmosphere in the solar system. Thus, we may be able to use Mars as another datapoint to build more accurate models of global climate and circulation. ReachBot can help answer questions about Mars's geologic evolution. The geologic record is often exposed in the form of steep, sub vertical outcrops that cannot be explored by traditional robots, but is specially targeted by ReachBot.

2.2 Science Objectives Beyond Mars

There is growing interest in missions that require robots capable of mobility and mobile manipulation under a variety of gravity regimes and terrain geometries that are not accessible to traditional robots. ReachBot's uniquely versatile design makes it amenable to scientifically valuable but challenging missions. For example, the Moon, in addition to Mars, has been identified as a key location to address science questions of the origin and evolution of terrestrial planets. In particular, the Moon's composition and internal structure – accessible through caves and lava tubes – hold a preserved history of the solar system. ReachBot's planetary cave exploration capabilities are crucial to characterize the Moon's morphology, stratigraphy, and topology. Additionally, ReachBot's versatile long reach provides advantageous mobility in low-gravity and microgravity missions, such as navigating an asteroid and space station servicing.

3 ReachBot Design, Development, and Experimentation

In this section, we present our study of ReachBot from conceptual design through prototype development and experimentation. We motivate ReachBot's design by introducing the numerous advantages of using extendable booms as robot arms (Section 3.1), then outline the challenges of this design and discuss how our control strategy addresses these challenges (Section 3.2). For simplicity, we demonstrate feasibility of ReachBot's capabilities by considering a 2D representation throughout the analysis. In Section 3.3, we describe our models for ReachBot's dynamics, one for each of two alternating stages of motion: body movement and end-effector movement. Then in Section 3.4, we present two waypoint-tracking controllers – one for each stage of motion – that jointly realize ReachBot's mobility. These controllers are demonstrated in simulation in Section 3.5. We then discuss the design and development of a gripper (Section 3.6) and full system prototype (Section 3.7). Finally, we share results from hardware experiments in Section 3.8. In each subsection, we discuss future research directions for following studies.

3.1 ReachBot Concept

3.1.1 Extendable Boom Concept

In contrast to traditional rigid-link robots, ReachBot provides a large reachable workspace through extendable booms. As shown in Figure 3.1, ReachBot's reachable space is larger than that of a comparably-sized rigid-link articulated-arm robot, increasing the number of accessible anchor points. Access to more anchor points grants ReachBot flexibility to choose between different anchoring options. This flexibility enables more secure grasp configurations, faster crawling speed, and less frequent re-planning, allowing ReachBot to move across terrain that might not be passable for other robots.

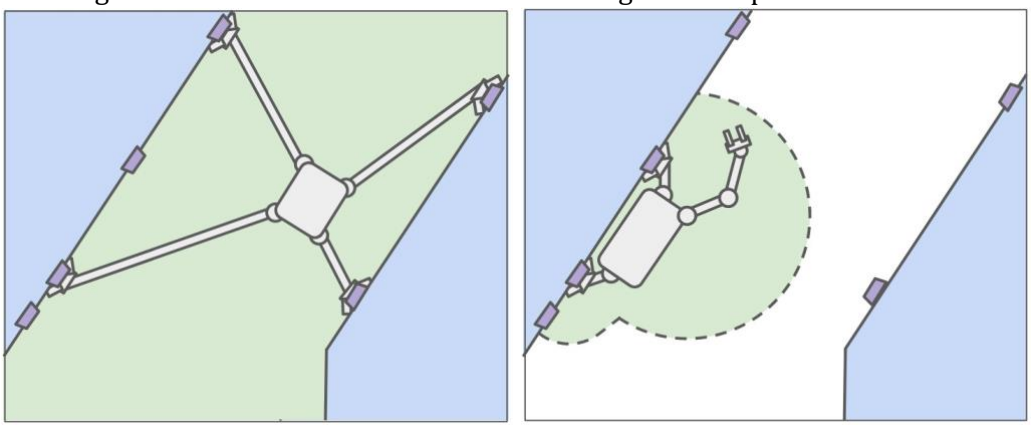

Figure 3.1: ReachBot (left) using its long reach to traverse terrain with sparse anchor points – shown in purple – that would inhibit an articulated arm robot (right). Each robot's reachable workspace is shown in green.

In addition to enhancing mobility, ReachBot's large reachable workspace provides advantages for manipulation. ReachBot uses its booms as tensile members to apply large wrenches on the environment, a strategy similarly exploited by small robots that anchor themselves and pull objects using tethers [25].

However, unlike tethers or cables, ReachBot's booms can be controllably extended, eliminating the need for the robot to move its body to each anchor point.

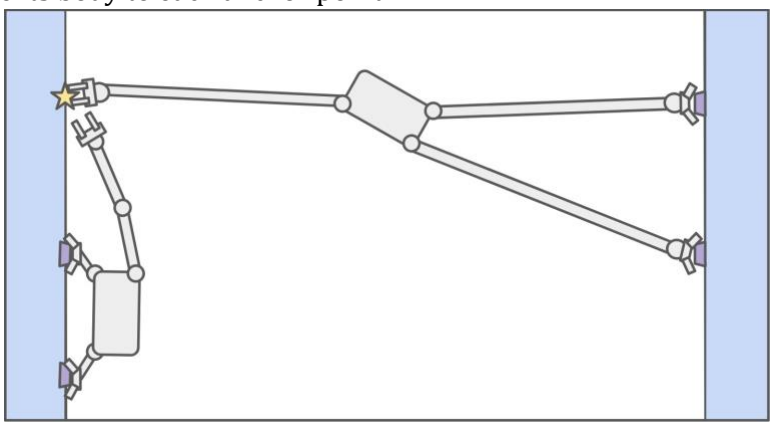

Figure 3.2: Alternative manipulation strategies to pull a target (yellow star) away from the wall. The lower, articulated-arm robot must anchor close to the target, then apply a large motor torque to lift its outstretched arm. ReachBot, shown above, completes the manipulation task with minimal lever arm and therefore minimal motor torque. It uses anchors on the opposite wall to apply a large manipulation force while keeping its booms under tension.

Figure 3.2 shows a scenario in which ReachBot is able to access a target that would be challenging for an articulated-arm robot. In particular, ReachBot requires fewer proximal anchor points and can reach the target from a much greater distance. Additionally, ReachBot performs a high-wrench manipulation task while using less torque than alternative strategies. Instead of depending on a large, powerful motor to apply torque and bending moment across a long lever arm, ReachBot uses anchors on an opposite surface to apply a force normal to the target surface while keeping its booms under tension.

Another key quality of ReachBot is that it achieves its numerous advantages within a lightweight and compact design. Due to the single-element uniform structure of the extendable booms, ReachBot's size, mass, and complexity do not scale significantly with increased reach, unlike comparable designs that rely on higher power consumption to actuate increasingly heavy rigid-link arms [11]. ReachBot's scalability provides several advantages for space robots, including reliability, reduced launch cost, and lower energy usage.

3.1.2 Future Work

Future work should conduct a trade study to determine the optimal 3D architecture of ReachBot, balancing the benefits of increased reach, such as a larger reachable workspaces, and the costs, such as reduced robustness. In particular, the trade study will consider parameters such as number and arrangement of booms, maximum extension of booms, number of active and passive actuators, and different payload requirements.

3.2 Structural Considerations

3.2.1 Overcoming Structural Challenges

Thin structural members like extended booms often have material properties that make them susceptible to buckling or bending failure. However, we can overcome typical limitations by applying

existing work in force closure for dexterous manipulators to exploit the booms' tensile strength.

In the field of multi-fingered dexterous manipulation, a robotic hand pushes on an object from multiple directions, manipulating it by applying forces at the contact points between the fingertips and the object. In this study, we considered an approach to ReachBot's mobility that is analogous to grasping with unisense contact forces [20, 26]: instead of having fingers that push, we have booms that pull. Many control strategies have been developed that enable a dexterous manipulator to follow a pose trajectory while maintaining force closure [27, 28]. Drawing parallels to this existing work, we can control ReachBot to achieve force closure by exploiting the concavity of surface geometry and establishing contact points in multiple directions.

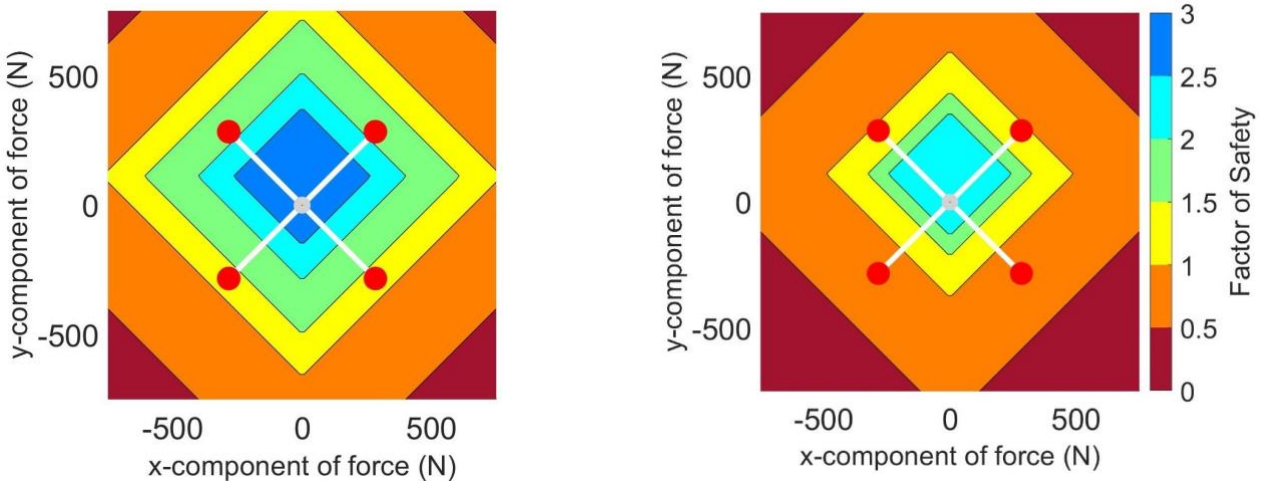

(a) With pretension

(b) Without pretension

Figure 3.3: The contours show ReachBot's minimum factor of safety while resisting different disturbances, where failure is expected for any factor less than 1 (orange and red). (a) With uniform pretension of 100*N* in all four booms, ReachBot has a larger factor of safety in the whole force space. (b) Without pretension, ReachBot has consistently lower factors of safety, making failure more likely.

By employing a force closure configuration, ReachBot exploits boom tensile strength to overcome typical design shortcomings of extendable booms, specifically their susceptibility to lateral disturbances and bending moments. Disturbances can be caused, for example, by an impulse due to a sudden grasp failure. Figure 3.3 demonstrates how ReachBot applies uniform pretension in its booms to reduce the likelihood of failure from disturbing forces. The figure illustrates ReachBot's factor of safety while resisting different disturbances in two scenarios: with and without applying pretension to the booms. Failure is expected for any factor less than 1 (shown in orange and red). In both cases, ReachBot's body configuration is stationary, and the *x* and *y* axes represent the *x* and *y* components of applied force, respectively. In addition to the applied force, ReachBot resists a constant downward (-*y*-direction) force of gravity. The contours in Figure 3.3 show the minimum factor of safety across all booms while resisting the total force, considering both buckling and yield failure. By leveraging the high tensile strength of the booms [29], ReachBot increases its robustness to disturbances. Figure 3.3(a) demonstrates a larger factor of safety across the whole force space when ReachBot applies a uniform pretension of 100*N* to all four booms. Figure 3.3(b) shows the same scenario without pretension, corresponding to lower factors of safety and therefore less ability to resist disturbances. ReachBot avoids significant bending forces by leveraging the booms' tensile strength to support its structure, a strategy that has been successfully demonstrated by cable-driven parallel robots [30].

3.2.2 Future Work

The next step in this investigation is to complete models for the limit surface of the booms and the grippers individually as well as their superposition to define an overall limit surface for the static system. For any applied wrench, such as a wrench involved in a mobility or manipulation task, the distance from that wrench to the edge of the limit surface determines the safety factor of that task, which can be used to define a quantitative robustness metric.

3.3 Model and Dynamics

Here we develop a model for ReachBot's dynamics and kinematics. First, in Section 3.3.1, we introduce and justify a series of assumptions that simplify the model, including a 2D planar adaptation of ReachBot that will be used throughout the report. We then break down ReachBot's motion into two alternating modes, mirroring a successful climbing paradigm for articulated-arm robots [11]. In Section 3.3.2, we consider the "body movement" stage, where all four of ReachBot's end-effectors remain anchored to the surface while the body moves in space. Then, in Section 3.3.3, we consider the "end-effector movement" stage where ReachBot detaches an end-effector and moves it to a new anchor point. By alternating these stages of motion, ReachBot can reposition its body and booms either to navigate within the environment or to ready itself for a manipulation task.

The result of this dynamical analysis is a set of equations that describe ReachBot's motion. These equations of motion define the relationship between applied joint torques (forces for prismatic joints) and resulting movement of the robot. For the duration of this section, we will refer to coordinate frames as defined in Figure 3.4. The frame C_r is fixed to the robot at its center of mass. The stationary frame C_w is fixed to the wall. The local wall frame C_{wi} is fixed relative to C_w with the origin at the point of contact with boom i, where the z-axis coincides with the wall's outward pointing normal. The shoulder frame C_{si} is fixed relative to C_r with its origin at the the base of boom i. The boom frame C_{bi} is fixed to boom i with its origin at the point of contact with the wall.

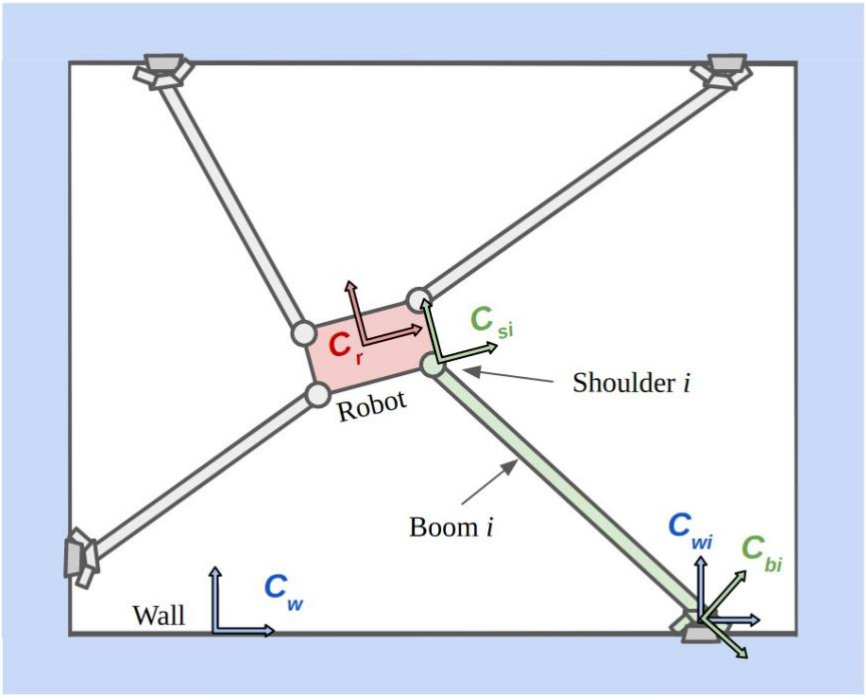

Figure 3.4: Coordinate frames for ReachBot in 2D. The frame C_w is fixed to the inertial wall frame, while C_r, C_s, and C_b correspond to the robot, shoulder joints, and booms, respectively.

3.3.1 Modeling Assumptions

We make a number of assumptions to simplify the modeling process. First, we assume we can ignore the dynamics of the booms and only consider the dynamics of the robot body and end-effectors. To support this assumption, we make two assertions: (1) the mass of the boom is negligible compared to that of the robot body and end-effector, which is consistent with our preliminary prototype, and (2) we can treat the boom as a rigid body. The latter is consistent with an analysis we performed whereby we compared pose estimates for rigid and flexible models of a fully extended boom with a 1kg end-effector mass and found less than a 1% deviation between the two models. By ignoring the boom dynamics, we simplify ReachBot's dynamical model while maintaining sufficient accuracy for a feasibility analysis.

Second, we assume the interaction between the end-effector and the wall can be modeled as a point contact having "embedded cone" friction [31], which is an idealization of the JKR friction/adhesion model [32]. This friction model sustains moderate pulling forces in the tensile direction while remaining attached to the wall.

Third, we assume there is a spring-loaded ball joint (a pin joint in the planar case) connecting the end of the boom to the gripper mount. The ball or pin joint ensures negligible moment at the contact while the spring keeps the joint from rotating freely, returning the end-effector to its equilibrium position when un-anchored.

Fourth, we assume the given trajectory can be executed with a series of stable, manipulable configurations. A configuration is said to be stable if, for every possible body wrench, there exists a choice of joint torques to balance it (up to joint torque limits). A configuration is manipulable if, for every body velocity direction, there is a choice of joint velocities that achieves the motion without breaking contact with the wall [27]. Because ReachBot remains within the convex hull of its end-effectors throughout the trajectory and has redundantly actuated controls, there must exist a trajectory where the configurations are stable and manipulable at all times during operation.

For simplicity, we use a 2D planar adaptation of ReachBot as a first step to validate the concept. This planar ReachBot adaptation includes a robot body with four shoulder mechanisms, each having two controllable joints: (1) a prismatic joint composed of a motor that extends and retracts the rollable boom and (2) a revolute joint that pivots the boom in the plane. Each boom assembly is capped with an end-effector. Eight independent control inputs (extension and rotation for each of four booms) give ReachBot full 3-DoF authority.

3.3.2 Body Movement Model

In this section, we present a dynamical model for ReachBot's body when all four end-effectors are anchored to the wall. Specifically, we pose this model as a set of equations that represent different constraints on ReachBot's motion. See [2] for the full derivation.

Dynamical constraints. ReachBot's dynamics are given by the Newton-Euler equation as

$$\begin{bmatrix} M & 0 \\ 0 & I \end{bmatrix} \begin{bmatrix} \dot{v}_{r,w} \\ \dot{\omega}_{r,w} \end{bmatrix} + \begin{bmatrix} \omega_{r,w} \times v_{r,w} \\ \omega_{r,w} \times I\omega_{r,w} \end{bmatrix} = \begin{bmatrix} f_r \\ \tau_r \end{bmatrix}, \tag{3.1}$$

where M is the mass of the robot body multiplied by the identity matrix in $\mathrm{R}^{3\times3}$, I is the inertia matrix with respect to the robot coordinates C_r, and $v_{r,w}$ and $\omega_{r,w}$ are the linear and rotational velocity, respectively, between coordinate frames C_r and C_w. Additionally, $[f_r,\tau_r]^\top$ is the resultant wrench (forces and torques) on the robot defined in the C_r frame. The resultant wrench directly causes motion, as opposed to the internal wrench, which is absorbed by the robot's mechanical structure.

Zero relative motion at contact. To ensure contact is maintained during manipulation, we enforce constraint equations for both relative velocities and wrenches between the robot and the contact points. The culmination of the derivation in [2] is a contact wrench constraint equation, found by combining contact wrench constraints for the four booms. It is given by

$$\begin{bmatrix} f_r \\ \tau_r \end{bmatrix} = \left[T_{w1,r}^{\top}, T_{w2,r}^{\top}, T_{w3,r}^{\top}, T_{w4,r}^{\top}\right] Gx, \tag{3.2}$$

where the grasp matrix G depends on the connection between the boom and the end-effector, which we model as a pin joint, allowing it to rotate freely in the plane and apply forces in all directions [33]. The matrix $T_{\alpha\beta}$ performs a generalized translation between coordinate frames α and β. Finally, the combined contact wrench vector for all four booms is given by x.

Static equilibrium at contact. Using the principle of virtual work, we derive a relationship between the joint torque vector τ and the contact wrench vector x. The resulting constraint is given by

$$\tau = J^{\top}x, \tag{3.3}$$

where J, the robot Jacobian, defines the relative velocity of the shoulder with respect to the body as a function of joint velocities.

3.3.3 End-Effector Movement Model

In the end-effector movement stage, ReachBot performs a maneuver that involves detaching an endeffector, moving the corresponding boom to a new position, and reattaching the end-effector to the wall. By tensioning the three anchored booms, we hold the robot body motionless. Thus we only need to consider the dynamics of a single boom, which we model as a massless rod with a point mass on the end.

3.3.4 Future Work

Future work should extend the existing model to three dimensions and account for the mass of the booms. Additionally, there should be further consideration on mobility methods that use compression as well as tension, leveraging the booms' small but non-zero compressive strength. One such strategy might use some of the booms as legs to walk along a flat surface under gravity. This opportunity for walking mobility distinguishes ReachBot's mobility capabilities from those of dexterous manipulators or cable-driven robots.

3.4 Control Strategy

In this section, we present two controllers that jointly realize ReachBot's mobility: one for the body movement stage and one for the end-effector movement stage.

3.4.1 Body Movement Control

Here we present a control scheme that enables ReachBot to follow a desired series of waypoints while maintaining wall contact with all four end-effectors. In [2], we modify a computed-torque controller designed for in-grasp dexterous manipulation to work for ReachBot. To simplify the relationship between force on the body and at the contacts given in (3.2), we define H as

$$H = \left[T_{w1,r}^{\top}, T_{w2,r}^{\top}, T_{w3,r}^{\top}, T_{w4,r}^{\top}\right] G. \tag{3.4}$$

The contact wrench needed to achieve a desired resultant wrench on the robot body is given by

$$x = H^{\dagger} \begin{bmatrix} f_r \\ \tau_r \end{bmatrix}, \tag{3.5}$$

where $H^{\dagger}$ is the left inverse of H, as defined in [2].

The objective of our controller design is to specify a vector of joint torque inputs τ to follow a desired series of waypoints given by

$$(p^d_{r,w}(t), A^d_{r,w}(t)) \in SE(3), \tag{3.6}$$

where $p^d_{r,w}$ and $A^d_{r,w}$ are the desired pose and orientation, respectively, of the robot with respect to the wall. We locally parameterize $A_{r,w} \in SO(3)$ by $\phi_{r,w}$, which represents the roll-pitch-yaw variables such that $\phi_{r,w} = [\phi_1, \phi_2, \phi_3]^{\top}$ is a nonsingular parameterization of $SO(3)$ [27]. Using this parameterization, we express desired waypoints as

$$(p^d_{r,w}(t), A_{r,w}(\phi^d_{r,w}(t))) \in SE(3), \tag{3.7}$$

and the body velocity as

$$\begin{bmatrix} v_{r,w}(t) \\ \omega_{r,w}(t) \end{bmatrix} = U(p_{r,w}(t), \phi_{r,w}(t)) \begin{bmatrix} \dot{p}_{r,w}(t) \\ \dot{\phi}_{r,w}(t) \end{bmatrix}, \tag{3.8}$$

where $U(p_{r,w}(t), \phi_{r,w}(t))$ is a matrix defined by the parameterization. In particular, U relates body velocity to the derivatives of the parameterization. We define the position error as

$$\begin{bmatrix} \widetilde{p} \\ \widetilde{\phi} \end{bmatrix} = \begin{bmatrix} p_{r,w} \\ \phi_{r,w} \end{bmatrix} - \begin{bmatrix} p^d_{r,w} \\ \phi^d_{r,w} \end{bmatrix}. \tag{3.9}$$

To realize the desired body acceleration $(\ddot{p}^d_{r,w}, \ddot{\phi}^d_{r,w})$ throughout the motion, we define the following control law based on feedback linearization

$$\begin{aligned} \tau = {} & J^{\top} H^{\dagger} \begin{bmatrix} M & 0 \\ 0 & I \end{bmatrix} \dot{U} \begin{bmatrix} \dot{p}_{r,w}(t) \\ \dot{\phi}_{r,w}(t) \end{bmatrix} \\ & + J^{\top} H^{\dagger} \begin{bmatrix} \omega_{r,w} \times M v_{r,w} \\ \omega_{r,w} \times I \omega_{r,w} \end{bmatrix} \\ & + J^{\top} H^{\dagger} \begin{bmatrix} M & 0 \\ 0 & I \end{bmatrix} U \left(\begin{bmatrix} \ddot{p}^d_{r,w} \\ \ddot{\phi}^d_{r,w} \end{bmatrix} - K_D \begin{bmatrix} \dot{\widetilde{p}} \\ \dot{\widetilde{\phi}} \end{bmatrix} - K_P \begin{bmatrix} \widetilde{p} \\ \widetilde{\phi} \end{bmatrix} \right), \end{aligned} \tag{3.10}$$

where K_P and K_D are proportional and derivative gain matrices. Both gain matrices must be positive definite. In [2], we verify that this control law will drive the error to zero with appropriate gains.

3.4.2 End-Effector Movement Control

The desired position for a single end-effector at the end of boom i is defined as the relative position of the C_{bi} frame with respect to the C_{si} frame. Tracking waypoints for the end-effector is accomplished using a standard PD controller

$$\begin{bmatrix} f_{bi} \\ \tau_{\theta i} \end{bmatrix} = K_P \begin{bmatrix} \widetilde{b}_i \\ \widetilde{\theta}_i \end{bmatrix} + K_D \begin{bmatrix} \dot{\widetilde{b}}_i \\ \dot{\widetilde{\theta}}_i \end{bmatrix}, \tag{3.11}$$

where the pose error is defined as

$$\begin{bmatrix} \widetilde{b}_i \\ \widetilde{\theta}_i \end{bmatrix} = \begin{bmatrix} b^d_i \\ \theta^d_i \end{bmatrix} - \begin{bmatrix} b_i \\ \theta_i \end{bmatrix}, \tag{3.12}$$

and f_{bi} and $\tau_{\theta i}$ are the prismatic force and revolute torque, respectively. The gain matrices K_P and K_D in (3.11) can be tuned separately for each stage of motion, so they are not necessarily the same as in (3.10). This control strategy does not rely on a model of ReachBot, but in future work we will design controllers that exploit the model developed in Section 3.3.3, for example a model predictive controller.

3.4.3 Future Work

Future work should design an optimized controller to maximize ReachBot's robustness throughout its trajectory based on the robustness metric described in Section 3.2.2. Experiments using 2D planar ReachBot prototype on the air-bearing granite table at the Stanford Space Robotics Facility should be conducted to test the trajectory optimization algorithm, evaluating both performance and computation requirements for replanning online. The next step would be to develop control strategies to mitigate risk due to dynamic failures. For example, model-predictive controllers have been demonstrated on cable-driven robots to reduce oscillations resulting from dynamic disturbances [34].

3.5 Simulation Results

3.5.1 Waypoint Tracking in Simulation

To showcase its unique ability to access challenging terrain, we deploy ReachBot in a simulated environment with sparse anchor points that would be impassible for existing robots. ReachBot follows a series of waypoints under nominal conditions, as well as with injected errors such as modeling errors and process disturbances that evoke common pitfalls of feedback linearization. By empirically demonstrating good performance under adverse conditions, we verify that our approach provides acceptable controllability.

The 2D simulation world is a hallway where the distance between the walls is less than the span of two of ReachBot's booms. Within the hallway, we define a discrete set of sparsely-spaced anchor points, with some adjacent anchor points up to several meters apart. The environment is defined this way such that a rigid-link articulated-arm robot would need to be prohibitively large to reach enough anchors to traverse the hallway. ReachBot's task is to move from one end of the hallway to the other.

ReachBot's two alternating stages of motion are illustrated in Figure 3.5(a) for body movement and Figure 3.5(b) for end-effector movement. Each waypoint defines a pose *either* for the robot body *or* a specific end-effector, therefore indicating the stage of motion at all times. The top-level planner uses a simple state machine to switch between the two controllers. This approach allows ReachBot to track the full series of waypoints, and will serve as a baseline for trajectory optimization development in future work.

Figure 3.6 shows an overview of ReachBot's full sequence of waypoints, as well as the nominal trajectory between waypoints. The waypoints are shown in yellow for the robot body and four separate colors for each of the four end-effectors. The figure delineates the starting position of ReachBot and its four end-effectors, then labels each waypoint in order of the sequence. The full sequence demonstrates the strategy of alternating body movement and end-effector movement to reach a desired final goal state, in this case waypoint 14.

In [2], we show that the computed torque feedback linearization controller from Section 3.4.1 converges quickly to each waypoint during body movement under nominal conditions. Additionally, we inject errors known to trigger pitfalls of feedback linearization. For example, computed torque controllers are often susceptible to modeling errors, so we investigate this potential concern by adjusting ReachBot's mass and inertia without changing the modeled values. ReachBot's controller must also be robust to process disturbances, so we similarly inject process noise and observe the system response. In some cases of injected error, we see slower convergence rates and minor overshoot

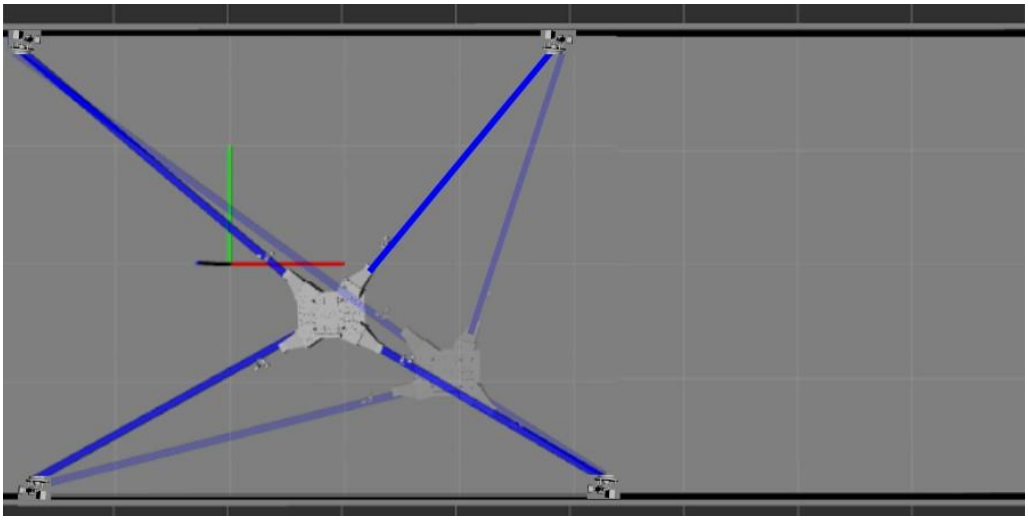

(a) Body movement stage

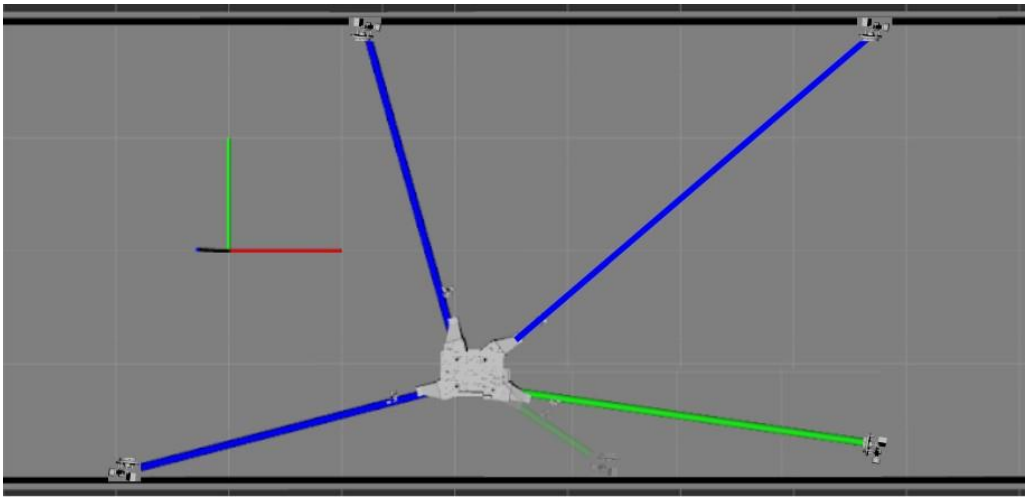

(b) End-effector movement stage

Figure 3.5: Snapshots of ReachBot simulation in different stages of motion. In the body movement stage (a), ReachBot's end-effectors remain anchored to the surface while the robot body moves in space. In the end-effector movement stage (b), ReachBot detaches an endeffector and moves it to a new anchor point. This mobility paradigm of alternating modes has been demonstrated successfully for articulated-arm robots [11].

in the response. However, in all cases, we observe the deviations decaying in reasonable time. Therefore, results from the simulation verify ReachBot's ability to follow a desired trajectory via a series of waypoints, even in the presence of modeling errors or process noise. With tuned gain matrices (K_P and K_D in (3.10) and (3.11)), ReachBot converges quickly to the nominal trajectory, minimizing the system's response time while avoiding both overshoot and overexerting the actuators.

3.5.2 Future Work

Future investigation will incorporate the 3D model of ReachBot into a 3D simulation. Additionally, simulation environments with irregular, cave-like geometries which approximate realistic settings will be created. For example, 3D depth maps of terrestrial caves are available to import into the simulation.

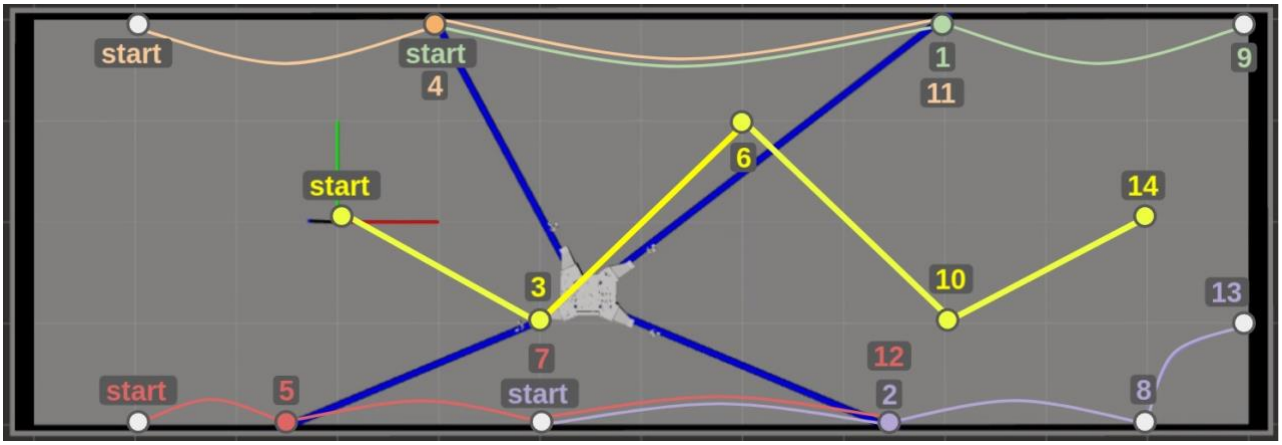

Figure 3.6: Overview of ReachBot traversing a full sequence of waypoints. Desired waypoints and nominal trajectory are shown in yellow for the robot body and four separate colors for each of the four end-effectors. The sequence of waypoints is labeled in order, demonstrating the strategy of alternating body movement and end-effector movement to move from a starting state to a goal state.

3.6 Gripper Design

Although ReachBot's booms are strong enough to extend and steer toward grip sites, they are vulnerable to buckling. In addition, the inertia that the rotational joints must drive will grow as mL^2 for a gripper of mass m and a boom of length L, and the boom oscillatory frequency will drop as $\sqrt{1/mL^3}$. These relationships make it essential to minimize gripper mass and minimize any tip reaction forces associated with securing and releasing a grasp. For these reasons we developed a new gripper with passive triggering and a remote reset located on the ReachBot body. This approach is a departure from the secure, but heavy, actuated spine grippers used in [11, 35] and similar climbing robots. In designing the new gripper, key questions include: How many spines are needed? What is the maximum pulling force? Over what range of orientations will it grasp reliably?

Fig. 3.7 shows that the gripper design depends on a number of interrelated factors, including the expected environment (e.g. how rough the surface is at multiple length scales) and interactions with other elements of the robot including the extending booms. Fig. 3.8 presents the new gripper design, including the compliant spine suspensions, the passive triggering mechanism, the reset function, and compliant wrist elements described in this section.

3.6.1 Surface Properties and Spines

Starting with the environment, the surface roughness and rugosity (waviness at macroscopic length scales) affect the size and number of required spines. It has been shown in previous work that maximum spine tip radius should be smaller than the average asperity (bump or pit) size on a surface [36, 19]. For the planar ReachBot prototype we use spines made from titanium-coated leather sewing needles (Organ Needles HAX130N) with a tip radius of approximately 10μm. Based on the analysis in [37], these spines should be able to support a maximum tangential force of approximately 20–30N each, depending on the rock surface.

Unlike robots designed for climbing concrete or stucco walls, ReachBot grips rock surfaces with macroscopic undulations and protrusions, which it can partially enclose between its fingers to provide some internal force perpendicular to the surface. At each spine, there is a force balance involving the contact forces (F_N, F_T), the corresponding grip force F_{grip}, and the pulling force F_{pull} (Fig. 3.8F). As a conservative estimate, F_N can be assumed to be close to 0, meaning that the spines can only

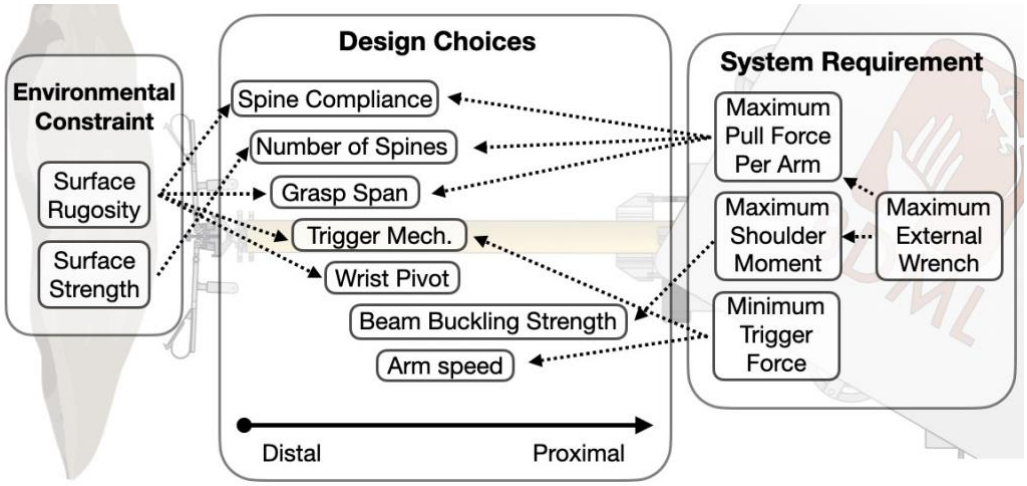

Figure 3.7: ReachBot gripper design depends partly on surface properties (roughness, rugosity, material strength) but is also tied to the design of other components including the extendable booms and pivoting wrist – for example, their ranges of motion and force capabilities.

apply forces tangential to the local surface. Then

$$F_{\text{pull}} = F_T \cos\phi, \tag{3.13}$$

where ϕ is defined by the radius of curvature. There are six spines on each of two fingers. Extrapolating from previous spine-based robots, we can assume conservatively that only half of the spines are typically engaged with asperities in the rock. With this assumption, we predict a maximum pull-out force of approximately 26N.

In practice, for the planar prototype, this force substantially exceeds both the mechanical strength of the 3D printed gripper parts and the maximum pulling force of the motor used to retract the booms. Thus the maximum pulling force in practice is approximately 8N.

An additional design consideration is to ensure the spines are long enough and have enough compliant suspension travel to reach into natural pits or valleys on the surface. Based on some experimentation with lava rocks, the spines are set at approximately 9mm shaft length, press fit into a 3D-printed housing, and secured with epoxy (Fig. 3.8A). This sets the angle of the spines with respect to the gripper finger to 45 degrees. The spine housing also serves as a connection to the spine suspension system which consists of two pieces of 0.127mm Kapton. The Kapton suspension is then glued to the fiberglass and 3D-printed base of the gripper finger. This provides each spine with approximately 10mm of vertical travel and 8mm of horizontal travel.

3.6.2 Gripper Trigger and Reset

As noted earlier, the gripper mechanism uses a passive design to keep its weight to a minimum. As the gripper approaches a surface, it makes initial contact with the spines at the tips of the jaws. The resulting contact forces align the gripper, rotating the passive compliant wrist joint at the base of the gripper (visible in Fig. 3.8C). We use rubber bands to bias the opposed fingers towards closing, as shown in Fig. 3.8B. The rubber bands are attached to an over-center mechanism with two stable positions: cocked and triggered. A plunger, visible in Fig. 3.8 in blue, depresses the mechanism as the gripper is propelled into a surface by the extending boom. The mechanism then snaps to the triggered configuration, where the rubber bands provide an internal force of approximately F_s = 2.5N. In practice, this has been found more than sufficient to achieve an adequate grip force on rounded protrusions; for nearly flat surfaces a higher grip force may be needed. To release a grasp, a small

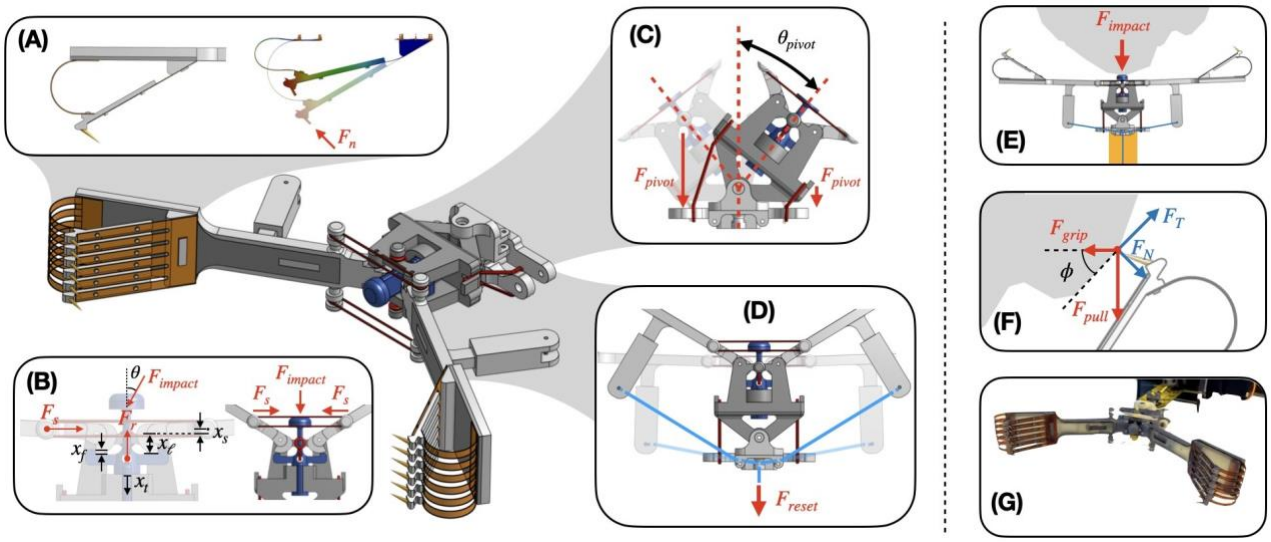

Figure 3.8: Detailed gripper mechanism and operation sequence. (A) shows the individual spine suspension through Kapton structures that provide both normal and linear compliance. (B) labels all relevant dimensions of the triggering mechanism and shows that the impact force releases the stored energy in the gripper. (C) shows the passive wrist joint of the gripper with restoring rubber bands that keeps the gripper in neutral position when unloaded. (D) displays the routing of the reset tendon. (E) shows the gripper triggering upon impacting a rock surface. (F) labels the force balance at each spine tip and (G) is a photo of the gripper.

motor and cable running along the boom pulls on the mechanism (F_{reset} in Fig. 3.8D), opening the mechanism and restoring it to the cocked configuration.

The contact force to trigger the gripper F_{required} is

$$F_{\text{required}} = \max(F_{\text{static}}, F_{\text{kinetic}}),$$

$$F_{\text{static}} = \frac{F_s x_s}{x_\ell}\mu_s + x_{t_i} k_t, \tag{3.14}$$

$$F_{\text{kinetic}} = \frac{F_s x_s}{x_\ell}\mu_k + (x_{t_i} + x_t) k_t, \tag{3.15}$$

where F_s is the gripper closing spring force, x_s is the lever arm for this closing force, x_ℓ is the lever arm with which the gripper finger exerts force on the trigger, x_t is trigger and finger mechanism overlap distance, μ_s and μ_k are the static and kinetic coefficients of friction of the gripper materials, and k_t is the spring constant for the trigger preload rubber band. Some of these variables are illustrated in Fig. 3.8B.

The ability to trigger the gripper also depends on the approach angle. To trigger the gripper, the impact force, F_{impact} must satisfy

$$F_{\text{impact}} \sin\theta > F_{\text{required}} + F_{\text{impact}}\mu_s \cos\theta, \tag{3.16}$$

where θ is the angle between the center line of the gripper and the direction of F_{impact} vector.

Given these considerations, Fig. 3.9 illustrates a plot of the force constraints associated with triggering the gripper overlaid with experimental data (see Section 3.8.1). The upper bound depends on the maximum impact force that the extending boom can provide. The lower bound is taken from F_{static} and F_{kinetic}. In practice, given the dimension of x_t, F_{static} is always greater. With the actual

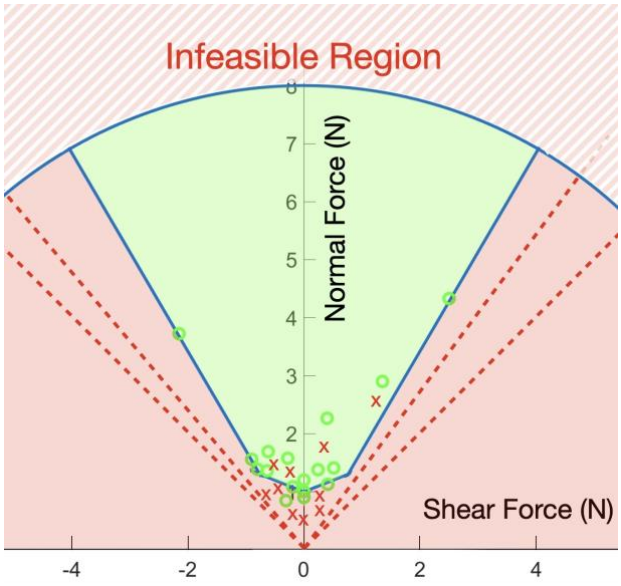

Figure 3.9: Forces required to trigger a grasp are bounded by maximum axial force the boom can apply (above), the minimum required force from (3.14) and (3.15) (below), and the effect of impact angle calculated by (3.16) (left and right). The light green shaded region represents impact forces predicted to trigger a grasp. Plotted circles show successful tests (Section 3.8.1); crosses show failures to grasp; dashed lines show failed approach directions.

dimensions of the gripper, the average F_{required} is 0.98N, within 10% of the calculated value of F_{static} from (3.14). The left and right bounds of the force space are determined by solving (3.16).

Once ReachBot is done maneuvering from a particular grasp point, it needs to be able to reset the gripper and prepare for the next grasp. As seen in Fig. 3.8D, two tendons, one attached to the back of each gripper finger, are merged into a single tendon at the gripper wrist which is pulled to perform the reset. Importantly, we extend the tendon attachment point out beyond each finger structure. This increases the lever arm of the resetting force, thus decreasing the required tension in the tendon needed to overcome the internal grasping force of the gripper. Additionally, it overcomes the geometric constraint that would occur when the revolute wrist joint is turned towards one side. Once the tendon system pulls the gripper fingers back to their horizontal positions, the spring on the quick-release pin pushes the pin into the armed state, preventing the grippers from closing again until the next grasp sequence.

3.6.3 Gripper Pivot

Each gripper is connected to a boom through a revolute joint, with rubber bands setting a spring equilibrium for the gripper at its center orientation, shown in Fig. 3.8C. This joint provides the gripper 90 degrees of rotational freedom with respect to the boom in the grasp plane and provides two key functions. First, it allows the gripper to passively align with the potential grasp surface when ReachBot is extending its boom. Second, once the gripper is securely engaged on the rock surface and ReachBot is retracting its boom to move, this degree of freedom minimizes the moment applied to the boom, keeping the boom in tension and minimizing bending moments imposed on the boom.

3.6.4 Future Work

The success of ReachBot depends on being able to identify candidate grasp sites and achieve secure attachments to them. These functional requirements, in conjunction with discoveries from the 2D

prototype built in Phase I, point future work towards three focus areas. The first is ReachBot's ability to scan rock surfaces in a three-dimensional space and characterize them to identify candidate locations with a high probability of providing a secure grasp. The second is the modeling of spinebased grasping of surface features to provide a reliable estimate of the maximum expected interaction forces as a function of surface properties, gripper mechanics, approach vector, and pulling angle. The maximum force and the probability of engagement also depend on gripper geometry and mechanics. Finally, the third is the design of new grippers for three-dimensional spine-based gripping while minimizing weight and power consumption. This design optimization will use a combination of numerical simulation and empirical validation on a three-dimensional test bed.

3.7 Boom Design and Prototype

During Phase I, we designed a planar prototype to test key components, notably the low weight grippers for grasping rock surfaces, and explore basic control strategies. Whereas the spatial version will be suspended by a combination of booms, as illustrated in Fig. 1.1, the planar version rolls on low friction ball transfer units (McMaster Carr 5674K64). It employs motorized contractor's tape measures as low-cost planar extending booms. Fig. 3.10 shows an overhead view of the planar prototype, as seen by a camera that tracks the positions of the robot body and each gripper, and the insets show how the gripper spines interact with rock samples. The goal of the planar prototype was to provide empirical data regarding gripper performance and insights for improving the gripper design, as well as testing control algorithms for coordinated movement of the booms and robot body.

3.7.1 Extendable and Pivotable Boom

As noted earlier, we use motorized contractor's tape measures (Black & Decker ATM100 Autotape) as low-cost planar booms. The tape measures behave similarly to extendable booms used for deployable space structures in that they are strong in tension and have some stiffness in other directions, though they are prone to buckling. Practically, this means the booms can handle enough compression and

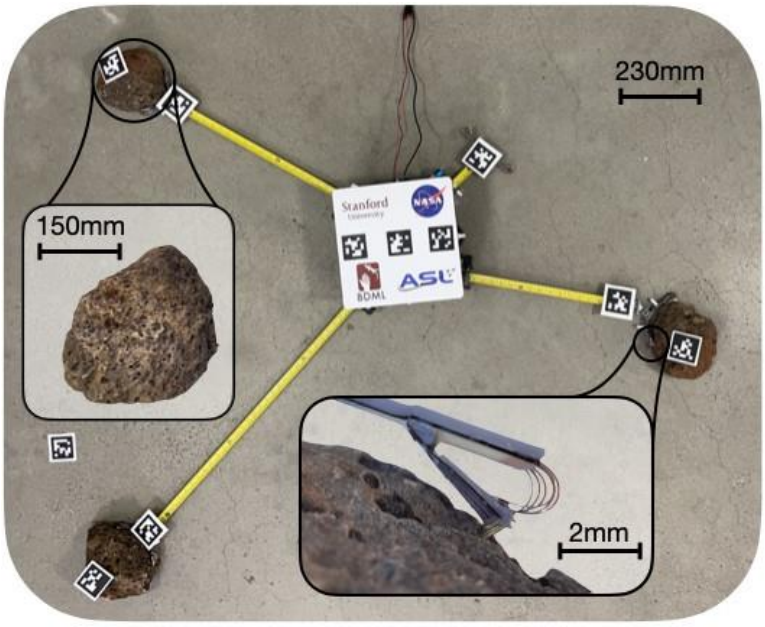

Figure 3.10: Overhead camera view of planar ReachBot prototype. Insets show enlarged detail of lava rock sample and gripper spines.

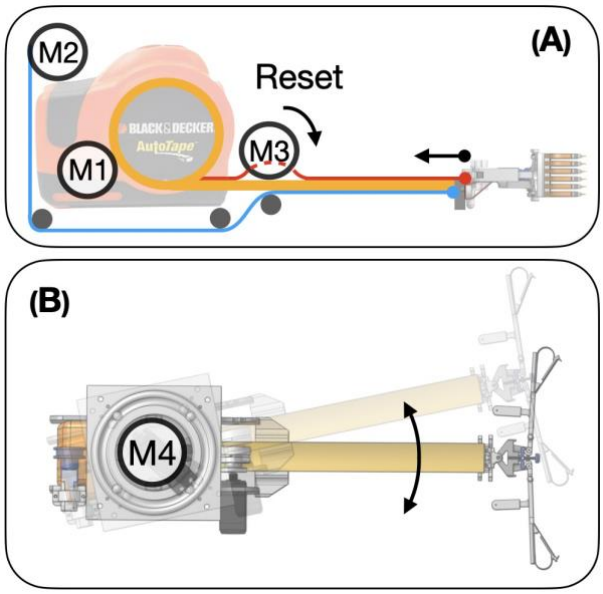

Figure 3.11: Each boom is controlled by four actuators. M1 is the original motor that extends and retracts the tape using a friction drive. M2 drives a winch that provides the maximum pull force. M3 is a small servo that controls the reset of the microspine gripper through a tendon. M4 controls the shoulder pivot.

bending forces to place the gripper on a specific target, unlike a tether or cable, then apply tension once attached.

The first challenge encountered while using these tape measures arises because they are driven using an internal DC motor (labeled M1 in Fig. 3.11A) through a friction drive that provides a low maximum pull force of 3.5N. To overcome this limitation, we add a second motor and winch (M2), which pulls a thin cable attached to the tape. With this motor, the maximum pulling force is 7N. An additional small servo (M3) is attached to a thin cable for resetting the gripper. This cable runs along the center of the tape (to minimize buckling) and winds up with the tape but can be pulled where it exits the tape measure body. When the gripper needs to be reset, M3 turns counter-clockwise, wrapping the tendon on the outside of a drum, thus pulling on the tendon. After resetting the gripper, the M3 servo rotates in the opposite direction to remove tension.

To enable coordinated movement, one more degree of freedom needs to be added at the base of the boom. This is accomplished by mounting each tape measure on a turntable bearing, controlled by an additional servo (M4 in Fig. 3.11B). This allows each boom to rotate up to ±35 degrees in the plane, from neutral. To reduce backlash, a biasing spring is used between each pivot and the base. Even so, angular errors propagate from the M4 servo to the boom tip so that it is necessary to use visual feedback to control gripper positions.

3.7.2 Kinematics and Control

Each boom of the planar ReachBot constitutes a serial R-P-R chain, of which the first two joints are actuated. These chains then operate in parallel on the robot body. As noted earlier, the problem of choosing grasp locations and controlling the boom forces is similar to grasping with a multi-fingered hand. In the planar prototype, we servo the shoulders to keep the booms aligned with the grasp targets. With this provision and the free pivot at the gripper, we can assume that bending moments are negligible

When searching for possible grasps, we first require that the system's configuration supports force closure. This problem is analogous to grasping with unisense contact forces [20, 26]: instead of having

fingers that push on an object, we have booms that pull. Four is the minimum number of unisense forces to achieve force closure in the plane [38].

Let $f = [f_1, f_2, f_3, f_4]^\top$ be a vector of the scalar force magnitudes along each of the booms and let $f_e = [f_{ex}, f_{ey}, m_e]^\top$ be a wrench corresponding to any external force and moment on the body, taken at its center of mass. The mapping from boom to body forces is then

$$G^\top f = f_e \tag{3.17}$$

where the grasp matrix $G^\top$ maps forces along the booms to the resultant force and moment. A condition of force closure is that $G^\top$, which depends on the grasp point locations, has full rank. In addition, we must satisfy upper and lower bounds on the forces:

$$f_{i,\min} \le f_i \le f_{i,\max} \tag{3.18}$$

Note that in principle $f_{i,\min}$ could be negative, corresponding to small compressive loads, in which case the permitted magnitude would vary inversely with boom length to prevent buckling. However, it is desirable to maintain a slight overall tension in the structure, hence $f_{i,\min}$ will typically be a small positive number, corresponding to a unisense constraint. The upper bounds $f_{i,\max}$ are based on the grip strength and will in general depend on the angle of the boom with respect to the rock, as well as the rock surface properties. Having satisfied equilibrium and grip constraints, we can minimize a function such as $f^\top f$ or $\sum f_i$, or for a safe grip, we could maximize the minimum distance of each grip force f_i with respect to its respective limit.

3.7.3 Future Work

The next step is to build a 3D prototype of a boom and gripper to be tested in a realistic mission context. To operate in 3D, the basic extensions to a 2D prototype include additional actuator degrees of freedom and the 3D gripper design. Further, unlike the 2D prototype built in Phase I, the 3D prototype must withstand gravitational loads. It must also be resilient to complications of real missions, such as dust permeating the boom's spool's inlet.

3.8 Experimental Results

To validate the functionality of both ReachBot's microspine grippers and the overall planar prototype, multiple bench-top tests and simulated environment demonstrations have been conducted. First, to validate the model of microspine and rock surface interaction and gripper design, the gripper was manually engaged with a red lava rock surface then the minimum triggering force and a sustained load were measured and applied by a force gauge. Then the ReachBot planar prototype was placed in an artificial environment with red lava rocks as potential grasping points, and key capabilities were demonstrated. From these experiments, we have validated our model and design and also gained insights into future needs in both sensing and control.

3.8.1 Gripping Experiments

Bench-top tests were conducted to evaluate the gripper. Forces were measured with a digital (Mark 10) force gauge and angles with a protractor. The results of approaching and gripping rock samples are plotted in Fig. 3.9, superimposed on the computed region for successful grasps. Forces and angles within the green region usually resulted in successful grasps while insufficient forces and excessive angles resulted in failures. The upper bound on force was limited by the boom extension motor and was not tested.

Maximum pull force could not be tested because it is limited by the strength of the 3D printed components and not by the spines. No grip failures occurred in tests with pulling forces limited to 8N.

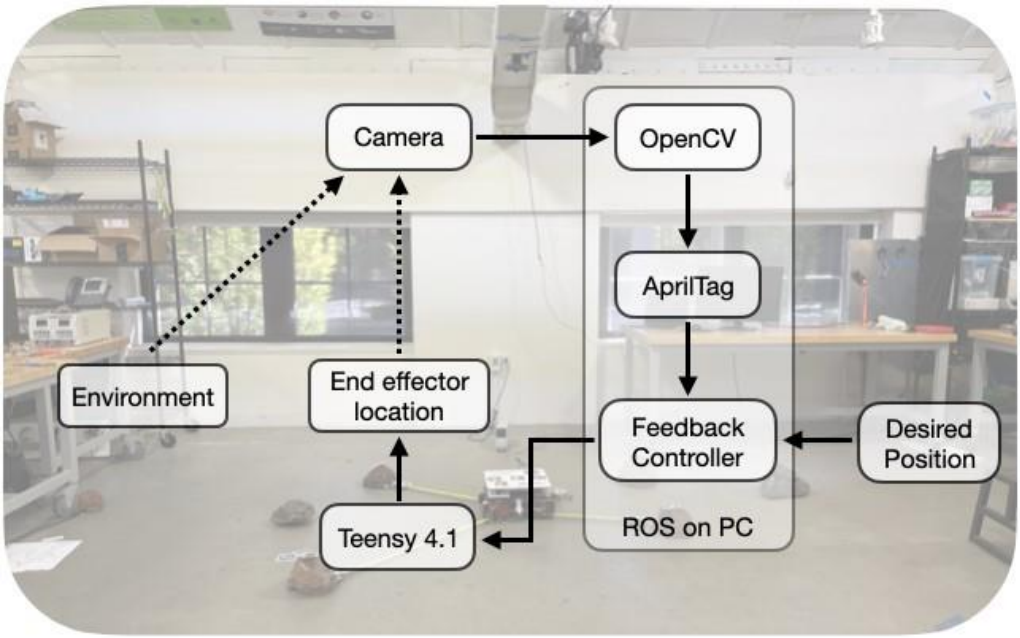

Figure 3.12: Experimental setup of closed loop control of ReachBot. Position of all environmental interests, robot body and end-effectors are labelled with AprilTags observed through a camera in bird's eye view. This ground truth, along with desired robot position, are fed into a feedback controller to determine the necessary motor commands.

3.8.2 System Demonstrations

The system schematic for demonstrations with the planar prototype is illustrated in Fig. 3.12. A Teensy 4.1 microcontroller on ReachBot receives ROS commands from the PC, enabling ReachBot to operate either with or without visual loop closure using a camera and AprilTags [39] to obtain ReachBot's true position and configuration with respect to a world frame. Based on this ground truth data, a simple feedback controller outputs motor commands to achieve a user-input desired position.

The first tests were to extend one of the booms of ReachBot toward a volcanic rock, triggering the gripper upon impact and then retracting the boom to pull the robot body (Fig. 3.13A). In these tests the gripper consistently achieved a secure grip sufficient to pull the body.

In a second test, three grippers were attached to three rocks, with a small initial tension in the three booms. A fourth boom then grasped another rock and pulls it toward the body (Fig. 3.13B). In this test the body remained stationary and the rock moved smoothly. A third open-loop test demonstrates the ability of the body to move in a line between two anchor points while maintaining grasps and some internal tension with two booms (Fig. 3.13C).

For closed loop control with vision, AprilTags [39] provide feedback on the locations and orientations of the robot body, the grippers and some target volcanic rocks. We showed in experiments (Fig. 3.13DF) that ReachBot is able to move the grippers to desired locations, identified with markers in the camera view, and then propel its body with coordinated extend-grasp-retract-release actions. A video of these demonstrations is included on the project website.

3.8.3 Discussion

The experiments validate the paradigm of passively-activated grippers at the end of extendable booms, but they also reveal several areas where we can improve on this design going forward. In particular, they highlight the following capabilities that will be required for multi-boom coordinated manipulation and eventual full autonomy.

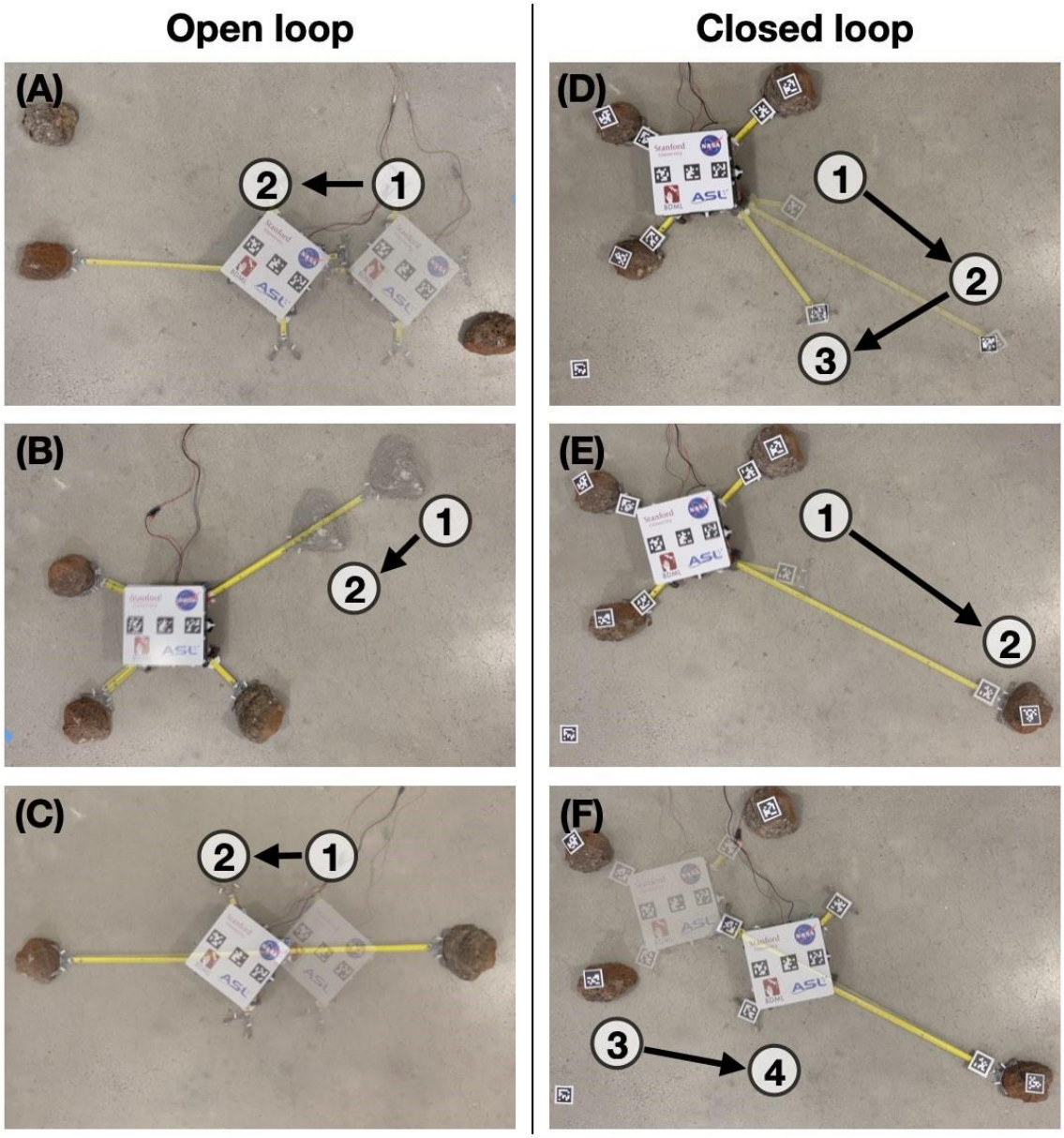

Figure 3.13: Open loop demonstrations of ReachBot: (A) single rock attachment and pull, (B) manipulation capability with multiple anchors and (C) two-boom coordinated movement. Closed loop visual control with AprilTags: (D) world frame end-effector positioning (E,F) locate rock, grasp, release anchor, and pull.

Contact sensing. Contact sensing is essential for coordinated movement in any manipulation task, but this prototype's lack of contact sensing has consequences unique to ReachBot's design. For example, when a boom extends out to grasp onto a rock, if it continues trying to extend past the point of contact, this extension force pushes backward on ReachBot, perturbing it and potentially causing one or more booms to buckle.

Control strategies. In this prototype, the extension and retraction of a boom are controlled by commanding relative position, while the revolute shoulder joint is commanded to absolute position. During experimentation, we noticed a discrepancy between the shoulder servo's internal pose estimate and the true position due to drift away from calibration. A small discrepancy in angle induces a large error in the gripper position at large extension. Therefore, this offset was the primary motivation for

incorporating visual feedback control, and it is a strong argument for relative position control in future iterations.

The experiments also suggest the potential need for force control of the servos, especially for extension and retraction. This will allow the control algorithm to define tension precisely for each boom and therefore pretension the booms to optimize grasp stability. To illustrate the effectiveness of pretensioning ReachBot's booms, we repeated the experiment shown in Fig. 3.13B *without* grasping the rock in the bottom-left corner. Despite their relatively weak buckling strength, the two booms stretched sideways with respect to the manipulated rock and, loaded in tension, provided enough stability to reel the rock in while keeping the body motionless.

3.8.4 Future Work

Future experiments using the 2D prototype should include testing the performance of trajectory optimization algorithms, applying loads near critical limits to validate the robustness metric, and inducing dynamic failures to validate oscillation reduction techniques. Further, future experiments should include testing a 3D prototype in a realistic environment such as a lava cave or cliff overhang. These tests should define operational requirements for ReachBot and determine the geological characteristics of a realistic mission, thus validating ReachBot's feasibility in a mission context.

4 Mission Architecture

In this section, we discuss mission objectives and the corresponding capabilities of ReachBot that help meet those objectives. We also identify possible payloads that address the scientific goals of ReachBot's mission. Then we consider a representative mission architecture to Huo Hsing Vallis, focusing on the unique geological features ReachBot may encounter and outlining operational tasks.

4.1 Mission Objectives and Reference Science Payload

The scientific goals proposed in NASA's Decadal Survey [4] and outlined in Section 1 require a comprehensive in-situ study of Martian caves and cliffs. The mission objectives to achieve these goals are to: (1) traverse rough terrain on the floor, walls, and ceiling, (2) investigate relevant scientific targets, and (3) record context of any measurements.

A detailed survey of a cavern interior and inspection of deeper stratified layers is critical to the success of such a mission. The terrain is likely to include overhanging surfaces, tight spaces, and expansive gaps. In addition to all the known obstacles, the interior topology of caverns is largely a mystery, requiring a robot capable of navigating obstacles and unexpected adverse terrain. Similar to cave-dwelling arthropods [40], ReachBot's long appendages allow it to overcome small-scale roughness while the slenderness of those appendages permits it to reach into tight places. ReachBot's design therefore makes it capable of retrieving a complete picture of Mars' stratigraphy by navigating the full breadth of the terrain and collecting data from every layer of bedrock.

In addition to mobility, investigating scientific targets requires a combination of remote sensing and contact observations. For example, remote sensing enables overall mapping of the walls at multiple wavelengths as well as identification of targets for closer investigation. ReachBot's remote sensing payload might consist of an IR navigation camera, a multispectral high-resolution color camera (building off the Mastcam-Z instrument onboard the Perseverance rover), or a hyperspectral imaging visible-shortwave infrared spectrometer to assess mineralogy. Mounting these instruments – all of which have been miniaturized to fit on spacecraft – to the ends of booms allows ReachBot to extend them much farther than its body can safely move. This capability enables overall mapping of cave or cliff walls, identifying targets for closer investigation, and studying inaccessible terrain such as tight crevasses.

Contact observations are also crucial for understanding the geological record. Contact instruments could include a microscopic imager, a DUV Raman spectrometer to detect potential organic molecules, and an X-Ray imaging spectrometer to map fine-scale elemental composition (building off the WATSON, SHERLOC, and PIXL onboard Perseverance, respectively) [41]. Larger robots like LEMUR perform bulk analysis, but centimeter-scale targets are key to characterizing geological, biological, and biochemical processes. ReachBot's small size and configurable booms allow it to place an instrument at a precise position relative to a target, for example to optimize the focal length of a microscope.

Lastly, subsurface exploration occludes direct access to solar power and communication. We address the challenge of subsurface power and communications by incorporating a tether for direct connection to the surface. In winding caverns, fixing tether redirects may be required, utilizing ReachBot's reach and wrench capability. Developing specifications for power, communication, and instrumentation subsystems is left to future work.

4.2 Case Study to Huo Hsing Vallis

We propose a mission architecture in the context of Huo Hsing Vallis, an ancient river valley with a canyon and a network of latticed ridges, pictured in Figure 4.1. Although a target site in the Huo Hsing Vallis may not be as protected from external factors as, for example, a lava tube with a small skylight entrance, a mission to Huo Hsing Vallis would benefit from reduced uncertainty by way of orbiter observation. Existing images confirm the large-scale terrain features, and high-resolution images could identify small-scale features and obstacles.

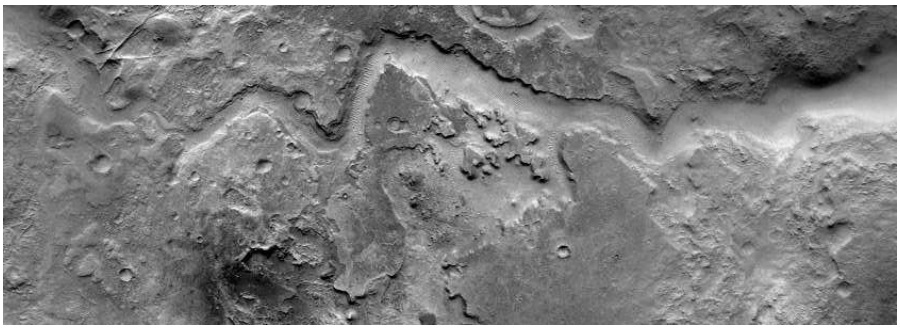

(a) Ancient river valley with dikes, layers, and dunes.

(b) Zoomed image of latticed ridges in upper left of **(a)**. Ridges are potentially caused by faults and underground water

Figure 4.1: Huo Hsing Vallis in Syrtis Major. Location is 27.8 degrees north latitude and 293 degrees west longitude.

We consider a mother-daughter mission architecture wherein a lander or rover on the surface anchors at the edge of the cliff and lowers ReachBot on a tether. At a high-level, the plan for mission operations includes two main phases:

A. **Surface craft anchors at the edge of a cliff.** Having a rover or lander on the surface provides numerous advantages to ReachBot's mission. Collaboration with a surface craft reduces ReachBot's mass by limiting the science payload that goes on the robot to sensors and sampling suites, leaving more bulky instruments such as X-ray (diffraction or fluorescence) or gas chromatograph on the surface. ReachBot could communicate to the surface through a tether, which provides not only communication and power channels, but could include a conveyor system that allows ReachBot to send physical samples back to the surface. More frequent transactions with the surface (and therefore updates to an orbiter and back to Earth) decreases the probability of data being lost in the case of a cave collapse or other catastrophic failure. Additionally, ReachBot could use a tether as an extra tensile member to increase stability.

B. **ReachBot traverses cliff walls while inspecting stratified layers.** ReachBot will navigate vertical and overhanging surfaces, as seen in Figure 4.2, by grasping anchor points. Unlike other climbing robots that can get stuck in cavernous terrain, ReachBot uses its long reach to avoid obstacles and cracks entirely. Inspecting and collecting data on stratified layers involves three reoccurring tasks:

1. *Collect data from crevasses.* While Earth is liberally coated in biological material, any potential biological material on other planets is likely to be hiding in protected environments such as deep inside crevasses or even ingrained in sedimentary material. In Figure 4.2(a), ReachBot reaches a boom-mounted instrument into a crack to take contact measurements.
2. *Drill, extract, and cache a sample.* A large reachable workspace allows ReachBot to assume stances that brace against forceful manipulation tasks, such as drilling to acquire samples for potential Earth return, as shown in Figure 4.2(b).
3. *Take a picture of the environment.* In Figure 4.2(c), ReachBot places its measurements in the context of its greater surroundings by taking a picture of its target site from an outstretched camera. One boom is always available for pointing/targeting without bearing load, reducing the bias on which surfaces ReachBot can observe in this way.

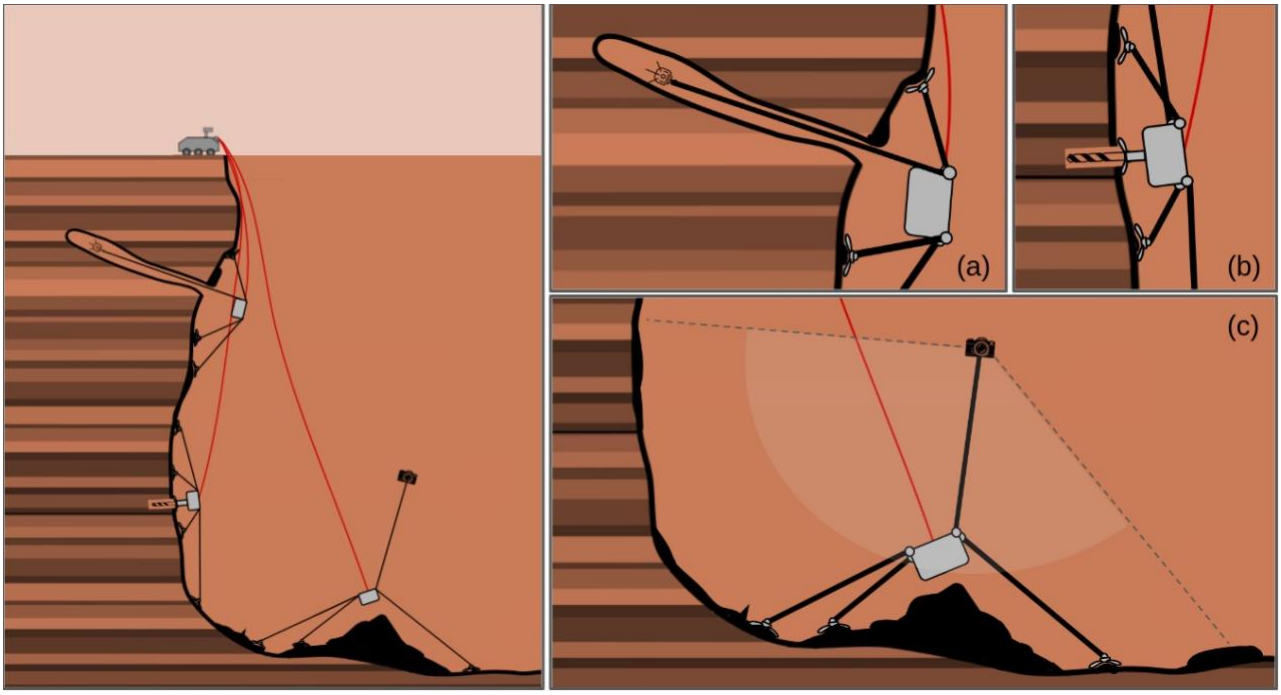

Figure 4.2: Martian mission concept sequence: ReachBot is lowered over a cliff via tether, uses its long arms to traverse the terrain and anchor to the wall, where it drills into stratified rock layers. Depiction includes features characteristic of terrestrial cliffs and caves, likely analogous to those on Mars.

4.3 Future Work

Future work will build on this architecture to develop a detailed mission procedure and define subsystem specifications grounded in this mission context. Additionally, a comparative study between ReachBot and other cave exploration robots will be performed, specifically looking at the science value and performance of robots in realistic cave scenarios.

5 Conclusions

In this effort we investigated a novel mission architecture for the exploration of difficult terrain on solar system bodies, with a key focus on subsurface caves and cliffs on Mars. Such a mission architecture is made possible by a long-reach crawling and anchoring robot that repurposes extendable booms for mobile manipulation. We demonstrated that the bounding assumptions behind our proposed robot design are reasonable, with a sound scientific and engineering basis. A future study should focus on the key feasibility and maturation aspects identified during Phase I, which can be grouped into four main categories:

- **Optimize the reachable workspace while maintaining a stable configuration.** This addresses ReachBot's ability to overcome the limitation of other robots and move around cavernous environments.
- **Develop a strategy to locate, select, and evaluate grasping sites that have a high probability of successful grasping with lightweight grippers.** This supports ReachBot's advantageous mobility paradigm that relies on autonomous detection and adherence to grasping sites on cave walls.
- **Design control strategies to mitigate risk.** This bolsters mission fulfillment, both by anticipating known risks and mitigating unpredictable risks.
- **Test the prototype in a realistic mission environment.** Outlining a detailed notional mission helps determine realistic operating constraints for ReachBot. Then, field tests can demonstrate the feasibility of the proposed concept for real-world deployments.

Acknowledgement: The research was carried out at Stanford University, under a contract with the National Aeronautics and Space Administration.

Bibliography

[1] G. E. Cushing. Mars global cave candidate catalog pds4 archive bundle. In *USGS Astrogeology Science Center*, 2017.

[2] S. Schneider, A. Bylard, T. G. Chen, P. Wang, M. R. Cutkosky, M. Lapôtre, and M. Pavone. ReachBot: A small robot for large mobile manipulation tasks. In *IEEE Aerospace Conference*, 2022. Submitted.

[3] T. G. Chen, B. Miller, C. Winston, S. Schneider, A. Bylard, M. Pavone, and M. R. Cutkosky. ReachBot: A small robot with exceptional reach for rough terrain. In *Proc. IEEE Conf. on Robotics and Automation*, 2022. Submitted.

[4] Space Studies Board, National Research Council, et al. *Vision and Voyages for Planetary Science in the Decade 2013-2022*. National Academies Press, 2012.

[5] L. Peterson, C. Nablo, D. Stringer, D. Tafoya, B. Stringer, P. Mahon, C. Emry, E. Strones, J. Garduno, T. Hamman, et al. Prototype for a caving robot drive mechanism to explore Mars. In *International Planetary Caves Conference*, 2015.

[6] J. Blank. Preparing for robotic astrobiology missions to lava caves on Mars: The BRAILLE Project at Lava Beds National Monument (N. CA, USA). *COSPAR Scientific Assembly*, 42:13— -18, 2018.

[7] I. A. D. Nesnas, J. B. Matthews, P. Abad-Manterola, J. W. Burdick, J. A. Edlund, J. C. Morrison, R. D. Peters, M. M. Tanner, R. N. Miyake, B. S. Solish, and R. C. Anderson. Axel and DuAxel rovers for the sustainable exploration of extreme terrains. *Journal of Field Robotics*, 29(4):663– 685, 2012.

[8] J. B. Matthews and I. A. Nesnas. On the design of the Axel and DuAxel rovers for extreme terrain exploration. In *IEEE Aerospace Conference*, 2012.

[9] R. Aoki, A. Oyama, K. Fujita, H. Nagai, M. Kanazaki, K. Kanou, N. Inoue, S. Sokabe, K. Tomisawa, and K. Uwatoko. Conceptual helicopter design for exploration of pit craters and caves on mars. In *AIAA SPACE Conferences & Exposition*, 2018.

[10] M. T. Pope, C. W. Kimes, H. Jiang, E. W. Hawkes, M. A. Estrada, C. F. Kerst, W. R. T. Roderick, A. K. Han, D. L. Christensen, and M. R. Cutkosky. A multimodal robot for perching and climbing on vertical outdoor surfaces. *IEEE Transactions on Robotics*, 33(1):38–48, 2017.

[11] A. Parness, N. Abcouwer, C. Fuller, N. Wiltsie, J. Nash, and B. Kennedy. LEMUR 3: A limbed climbing robot for extreme terrain mobility in space. In *Proc. IEEE Conf. on Robotics and Automation*, 2017.

[12] P. Hebert, M. Bajracharya, J. Ma, N. Hudson, A. Aydemir, J. Reid, C. Bergh, J Borders, M. Frost, M. Hagman, J. Leichty, P. Backes, B. Kennedy, P. Karplus, B. Satzinger, K. Byl, K. Shankar, and J. Burdick. Mobile manipulation and mobility as manipulation—Design and algorithms of RoboSimian. *Journal of Field Robotics*, 32(2):255–274, 2015.

[13] R. O. Ambrose, H. Aldridge, R. S. Askew, R. R. Burridge, W. Bluethmann, M. Diftler, C. Lovchik, D. Magruder, and F. Rehnmark. Robonaut: NASA's space humanoid. *IEEE Intelligent Systems and their Applications*, 15(4):57–63, 2000.

[14] C. S. Hazelton, K. R. Gall, E. R. Abrahamson, R. J. Denis, and M. S. Lake. Development of a prototype elastic memory composite STEM for large space structures. In *Structures, Structural Dynamics, and Materials Conference*, 2003.

[15] C. Leclerc, L. Wilson, M. A. Bessa, and S. Pellegrino. Characterization of ultra-thin composite triangular rollable and collapsible booms. In *AIAA SPACE Conferences & Exposition*, 2017.

[16] M. Whorton, A. Heaton, R. Pinson, G. Laue, and C. Adams. NanoSail-D: The first flight demonstration of solar sails for nanosatellites. In *AIAA/UTU Small Satellite Conference*, 2008.

[17] B. R. Spence, S. White, M. LaPointe, S. Kiefer, P. LaCorte, J. Banik, D. Chapman, and J. Merrill. International Space Station (ISS) Roll-Out Solar Array (ROSA) spaceflight experiment mission and results. In *IEEE World Conf. on Photovoltaic Energy Conversion*, 2018.

[18] A. T. Asbeck and M. R. Cutkosky. Designing compliant spine mechanisms for climbing. *Journal of Mechanisms and Robotics*, 4(3):1–8, 2012.

[19] H. Jiang, S. Wang, and M. R. Cutkosky. Stochastic models of compliant spine arrays for rough surface grasping. *Int. Journal of Robotics Research*, 37(7):669–687, 2018.

[20] A. Bicchi and V. Kumar. Robotic grasping and contact: A review. In *Proc. IEEE Conf. on Robotics and Automation*, 2000.

[21] A. M. Okamura, N. Smaby, and M. R. Cutkosky. An overview of dexterous manipulation. In *Proc. IEEE Conf. on Robotics and Automation*, 2000.

[22] T. Yoshikawa. Multifingered robot hands: Control for grasping and manipulation. *Annual Reviews in Control*, 34(2):199–208, 2010.

[23] Mathieu GA Lapôtre, Joseph G O'Rourke, Laura K Schaefer, Kirsten L Siebach, Christopher Spalding, Sonia M Tikoo, and Robin D Wordsworth. Probing space to understand earth. *Nature Reviews Earth & Environment*, 1(3):170–181, 2020.

[24] M.G.A. Lapôtre, J.L. Bishop, A. Ielpi, D.R. Lowe, K.S. Siebach, N.H. Sleep, and S.M. Tikoo. Mars as a time machine to precambrian earth. *Geological Society, London, Special Publications*.

[25] M. A. Estrada, S. Mintchev, D. L. Christensen, M. R. Cutkosky, and D. Floreano. Forceful manipulation with micro air vehicles. *Science Robotics*, 3(23):1–7, 2018.

[26] L. Han, J. C. Trinkle, and Z. X. Li. Grasp analysis as linear matrix inequality problems. *IEEE Transactions on Robotics*, 16(6):663–674, 2000.

[27] Z. Li, P. Hsu, and S. Sastry. Grasping and coordinated manipulation by a multifingered robot hand. *The International Journal of Robotics Research*, 8(4):33–50, 1989.

[28] K. Nagai and T. Yoshikawa. Dynamic manipulation/grasping control of multifingered robot hands. *Proc. IEEE Conf. on Robotics and Automation*.

[29] J. M. Fernandez. Advanced deployable shell-based composite booms for small satellite structural applications including solar sails. In *4th International Symposium on Solar Sailing*, 2017.

[30] M. Carricato and J. Merlet. Stability analysis of underconstrained cable-driven parallel robots. *IEEE Transactions on Robotics*, 29(1):288–296, 2012.

[31] D. Soto, A. Parness, N. Esparza, T. Kenny, K. Autumn, and M. R. Cutkosky. Microfabricated dry adhesive displaying frictional adhesion. In *Hilton Head 2008 solid state sensors, actuators, and microsystems*, 2008.

[32] K. L. Johnson, K. Kendall, and A. D. Roberts. Surface energy and the contact of elastic solids. *Proceedings of the royal society of London. A.*, 324(1558):301–313, 1971.

[33] J. Kerr and B. Roth. Analysis of multifingered hands. *The International Journal of Robotics Research*, 4(4):3–17, 1986.

[34] Imane Khayour, Sylvain Durand, Loïc Cuvillon, and Jacques Gangloff. Active damping of parallel robots driven by elastic cables using on-off actuators through model predictive control allocation. *IFAC-PapersOnLine*, 53(2):9169–9174, 2020.

[35] W. Ruotolo, F. S. Roig, and M. R. Cutkosky. Load-sharing in soft and spiny paws for a large climbing robot. *IEEE Robotics and Automation Letters*, 4(2):1439–1446, 2019.

[36] A. T. Asbeck, S. Kim, M. R. Cutkosky, W. R. Provancher, and M. Lanzetta. Scaling hard vertical surfaces with compliant microspine arrays. *Int. Journal of Robotics Research*, 25(12):1165–1179, 2006.

[37] S. Wang, H. Jiang, and M. R. Cutkosky. Design and modeling of linearly-constrained compliant spines for human-scale locomotion on rocky surfaces. *Int. Journal of Robotics Research*, 36(9):985–999, 2017.

[38] X. Markenscoff, L. Ni, and C. H. Papadimitriou. The geometry of grasping. *Int. Journal of Robotics Research*, 9(1):61–74, 1990.

[39] E. Olson. AprilTag: A robust and flexible visual fiducial system. In *Proc. IEEE Conf. on Robotics and Automation*, 2011.

[40] T Delić, P Trontelj, V Zakšek, and C Fišer. Biotic and abiotic determinants of appendage length evolution in a cave amphipod. *Journal of Zoology*, 299(1):42–50, 2016.

[41] Kenneth H Williford, Kenneth A Farley, Kathryn M Stack, Abigail C Allwood, David Beaty, Luther W Beegle, Rohit Bhartia, Adrian J Brown, Manuel de la Torre Juarez, Svein-Erik Hamran, et al. The nasa mars 2020 rover mission and the search for extraterrestrial life. In *From habitability to life on Mars*, pages 275–308. Elsevier, 2018.